Coordination Chemistry Reviews 380 (2019) 17–34

Contents lists available at ScienceDirect

Coordination Chemistry Reviews

journal homepage: www.elsevier.com/locate/ccr

Review

Organic fluorescent probes for stochastic optical reconstruction microscopy (STORM): Recent highlights and future possibilities

Soham Samanta [a,1], Wanjun Gong [a,1], Wen Li [a], Amit Sharma [b], Inseob Shim [b], Wei Zhang [a], Pintu Das [a], Wenhui Pan [a], Liwei Liu [a], Zhigang Yang [a,*], Junle Qu [a,*], Jong Seung Kim [a,b,*]

[a] Key Laboratory of Optoelectronic Devices and Systems of Ministry of Education and Guangdong Province, College of Optoelectronic Engineering, Shenzhen University, No. 3688, Nanhai Boulevard, Nanshan District, Shenzhen 518060, China
[b] Chemistry Department, Korea University, Seoul 02841, Republic of Korea

ARTICLE INFO

Article history:
Received 26 June 2018
Accepted 7 August 2018
Available online 11 October 2018

Keywords:
STORM/dSTORM
Organic fluorophore dyes
Photo-switching
Multicolor STORM imaging
Live cell STORM imaging

ABSTRACT

Super-resolution fluorescence imaging by single-molecule localization microscopy (SMLM) offers the possibility of microscopic images with sub-diffraction spatial resolution. Stochastic optical reconstruction microscopy (STORM) is one of the emerging SMLM techniques that has contributed new insights into both the structures and functions of sub-cellular organelles in the cellular context with a spatial resolution virtually at the molecular level. Photo-switching of single fluorophores and position determination are the most common features of this SMLM technique, which allows molecule-resolved information as well as super-resolved images. However, achieving successful STORM-based images relies on the suitable choice of a fluorophore. In particular, the use of ideal organic fluorescent probes has great potential to circumvent common difficulties that arise during the construction of STORM images. However, there is hardly any comprehensive review that critically assesses the criteria for choosing ideal fluorescent probes for STORM and designing new efficient organic fluorescent probes to date. Therefore, this review has particularly focused on the choice of organic fluorescent probes, the essential features for designing new probes and the future prospects for resolving persistent issues in STORM imaging. The utility of organic fluorescent probes in multicolor STORM, 3D STORM and live cell STORM imaging are also discussed to provide a perspective concerning the true application potential of commonly used fluorescent dyes. In this review, we not only describe how organic fluorescent dyes have contributed to the growth of STORM-based super-resolution imaging in eukaryotic biology, but we also attempt to provide a basis on which advanced organic fluorescent probes can be designed and developed in the near future.

Contents

* Corresponding authors at: Chemistry Department, Korea University, Seoul 02841, Republic of Korea (J.S. Kim).
E-mail addresses: zhgyang@szu.edu.cn (Z. Yang), jlqu@szu.edu.cn (J. Qu), jongskim@korea.ac.kr (J.S. Kim).
[1] These authors made equal contributions.

https://doi.org/10.1016/j.ccr.2018.08.006
0010-8545/

1. Introduction

Over the last century, light microscopy has been widely used in biomedical research because of its non-invasive nature [1–3]. However, the resolution of a light microscope is limited by the diffraction limit, as defined by Abbe's law of diffraction, and the best possible resolution that can be achieved in a conventional microscope using visible light is approximately ~180 nm in the lateral direction and ~500 nm in the axial direction. To surpass the resolution limit, several approaches have been adopted by various scientists in recent decades. For instance, scanning tunneling microscopy has been successfully utilized for imaging of subcellular structures, such as mitochondria and lysosomes. However, these technologies have failed to gain much attention from biologists because of their low depth of penetration, inability to image live cells and thick samples. Hence, the development of new non-invasive high-resolution microscopy techniques that can provide detailed information about ultra-small size organelles in living cells is highly anticipated. In this context, various super-resolution microscopy techniques have been developed over the years that allow users to acquire nano-scale information concerning objects in living cells. Super-resolution image techniques can be generally divided into two classes; (i) near-field optical microscopy and (ii) far-field microscopy. Near-field scanning optical microscopy (NSOM) [4] is mostly used to study surfaces, whereas far-field microscopy includes interferometric techniques, such as structured illumination microscopy (SIM) [5], saturated structured illumination microscopy (SSIM) [6], stimulated emission depletion (STED) [7,8], photo-activation localization microscopy (PALM) [9], stochastic optical reconstruction microscopy (STORM) [10] and fluorescence photo-activation localization microscopy (fPALM) [11].

Two different approaches can be used to obtain super-resolution images; these are single-molecule localization microscopy (SMLM) and reversible saturable optical fluorescence transitions (RESOLFT) microscopy. Microscopic techniques like stochastic optical reconstruction microscopy (STORM), photo-activation localization microscopy (PALM) and fluorescence photo-activation localization microscopy (fPALM) are part of SMLM, whereas RESOLFT comprises stimulated emission depletion (STED) microscopy, ground state depletion (GSD) microscopy and saturated structured illumination microscopy techniques. STORM, as a representative of SMLM, has received increased attention in recent years and hence has provided strong contributions to fluorescence-based super-resolution microscopy techniques for studying cellular and molecular biology in depth.

However, the field of super-resolution microscopy as a whole, and especially STORM microscopy as one of its most promising techniques, remains a very young research topic that requires careful nurturing. In this context, a timely review and a deep understanding of the subject are essential to enrich the active field of research. Although some review articles [12–15] have articulated the conceptual basis of SMLMs and advancements in the technical methods, they have hardly shed any light on the progress in designing newer fluorescent probes for SMLMs. Most of the super-resolution microscopy and/or STORM related discussions very broadly deliberate upon the probe selections and scarcely include details of structural illustrations with contemporary applications [16–18]. Hence, in this review, we primarily attempt to elaborate the use of several organic fluorophores in STORM/dSTORM and their utility in probing subcellular organelles by surpassing the diffraction limit. In addition to highlighting the use of various fluorophores, a genuine effort is made to provide criteria/grounds on which ideal fluorescent probes can be chosen or developed for future STORM-based advanced studies. We believe that a comprehensive review, particularly focusing on the use of small molecule-based organic fluorophores, will be helpful to the scientific community at large who are involved in the active field of STORM/dSTORM imaging.

2. The basic concept of STORM

Fluorescence microscopy (FM) has become an indispensable aspect of biomedical research because of its simple wide-field image processing ability and the ability to use live cells [19–24]. However, conventional fluorescence microscopy is limited by the diffraction barrier, as mentioned earlier. When the distance between two image spots becomes smaller than the radius of the Airy disk, FM cannot identify each of those image spots separately, which eventually leads to indistinguishable image spots with considerable overlap. However, this situation can be prevented if the two fluorophore molecules at two different spots emit consecutively rather than concurrently. In that case, the location could be determined using a centroid localization algorithm and Gaussian fitting methods without altering the radius of the Airy disk, as each image spot would be attributed to a single fluorescent molecule. However, this strategy may not be able to provide accurate location information, and because the accuracy is related to the detected photon quantity, it can have direct implications on the size of the image point [25]. Basically, soon after imaging, the profiles are reconstructed with the same technology, so that the two almost indistinguishable image points become worth identifying. This constitutes the common basic concept of single-molecule localization-based super-resolution technology (Scheme 1; left).

Even though a common concept is utilized in various super-resolution microscopy technologies, the process of switching between fluorescent and dark (non-fluorescent) states can vary substantially in different SMLM techniques, which provides the opportunity for specific implementation for diverse imaging purposes. However, as the current discussion particularly focuses on STORM, the basics of STORM microscopy will be briefly illustrated here.

In Scheme 1 (right), the STORM imaging method and its principle is conveniently illustrated. The basic principle of this method is to determine the positions of the fluorescent labels in a sample (labelled with proper fluorescent probes) and then to plot the image spots to obtain a complete image. As mentioned above, the imaging process comprises multiple cycles. In the meantime (during these multiple cycles), the fluorophores are activated, imaged and deactivated continuously. However, to allow each fluorophore to be localized with high precision, the density of the activated molecules is maintained using a weak activation light intensity in such a way that the images of the individual fluorophores do not overlap. Repetition of this process results in the activation of a stochastically different subset of fluorophores in each cycle, which ultimately helps to determine the positions of

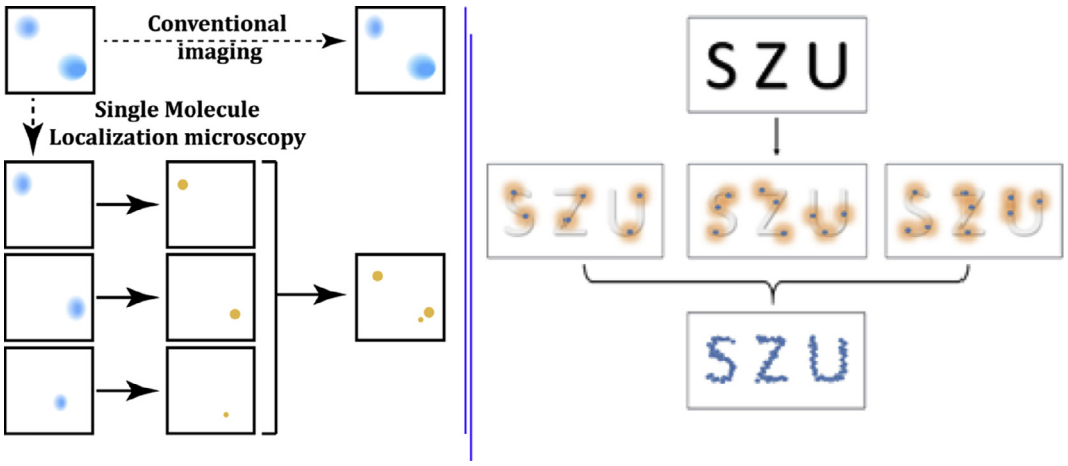

Scheme 1. Schematic representation of the basic principle of SMLM imaging (left) and the typical method of STORM imaging generation (right).

the fluorophores. After recording a sufficient number of localizations, a high-resolution image can be constructed from the measured positions of the fluorophores. Hence, the resolution of the final image obtained by this method is not limited by diffraction; rather, the precision of localization and the localization density are the two main factors that determine the resolution. In other words, the resolution of the image depends on the number of photons collected from the fluorophores and the number of fluorophores used for labelling of the sample. This microscopic method has been widely termed "stochastic optical reconstruction microscopy," and during its first implementation, a dye-pair approach was used. The activator, that is primarily responsible for activating the fluorescence randomly, and the reporter, that is responsible for generating the signal, together play vital roles in achieving the process successfully. The reporter becomes fluorescent upon excitation with an imaging laser, whereas it can be turned in to a non-fluorescent state using an imaging buffer. A neighboring reporter dye molecule then becomes fluorescent when the activation laser is utilized to simulate the activator [26]. The acquisition of imaging data becomes possible when a subset of the reporter fluorophore dyes becomes fluorescent.

3. Essential criteria for designing organic fluorescent probes for STORM

The photophysical and photochemical properties of fluorescent probes are important for all kinds of fluorescence imaging, including super-resolution imaging. Fluorescence technology is preferred over other techniques when a fast response and high sensitivity are critical. In this context, the choice of a suitable fluorophore must satisfy some essential criteria to potentially be utilized in STORM. There are three different types of fluorescent probes commonly used for STORM imaging, including (a) organic small molecule probes, (b) fluorescent proteins and (c) semiconductor crystal quantum dots (Fig. 1).

Generally, conjugated electronic π-systems comprising both aromatic rings as well as C═C, C═O or N═N bonds are used as the chromophore backbones for the organic dyes in STORM imaging. Hence, the fluorogenic behavior of the fluorescent probes can be significantly influenced by several structural features, like the number of electrons, substituents and the extended π-conjugation. To pursue effective bio-imaging, it is important to match the excitation and emission wavelength range of the chosen organic fluorophore with that of the given microscopic system. It should be noted that each organic fluorophore system contains a particular excitation and emission wavelength range, so the choice of fluorophore should be in accordance with the experimental requirements. Even though quantum dots possess convenient wide but strong absorptions because of their confined size [27], the discussion in this article will be mostly limited to organic dyes. Reversible photoswitchable fluorescent proteins are also excluded from this review, as they have already been thoroughly discussed by Shcherbakova and Adam et al. [28,29].

As mentioned earlier, single-molecule localization-based super-resolution imaging can conveniently surpass the limit of optical diffraction. However, without choosing an apt fluorophore, high-quality super-resolution imaging cannot be achieved. If a fluorogenic system can transition between fluorescence ***on*** and ***off*** states, or in other words, it can switch between the fluorescent and non-fluorescent state alternatively, then the system can possibly be employed in STORM. However, an organic probe only capable of demonstrating switching behavior is not good enough to procure

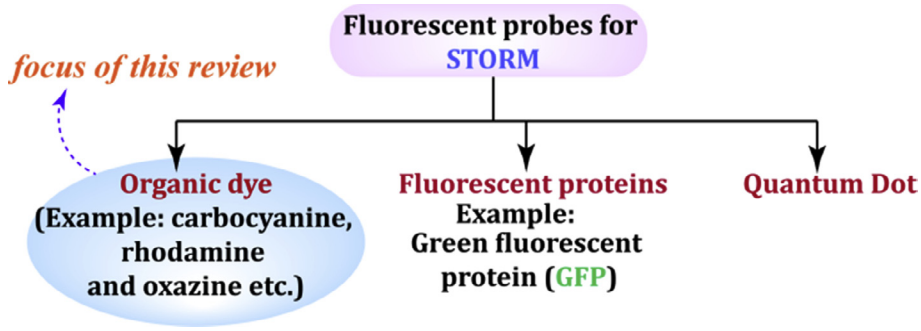

Fig. 1. Types of fluorophores used in STORM and the focus of this review.

a high-resolution image. It is important to make only some of the fluorophores emit at a time, while most of the fluorophores remain in the "off" state, so that the possibility of two molecules existing under the diffraction limit at the same time becomes minimal. As a result, the obtained image spots at every occasion should correspond to the set of a single molecule only. A large number of images containing distinct image spots can then be obtained by repeating the imaging procedure, and the super-imposition of those images can result in a complete super-resolution image.

The brightness of the molecules in the fluorescent state (used for localization) and the ratio between the brightness of this state to the molecules in the non-fluorescent state are the two most important photophysical factors that determine the spatial resolution. The brightness of the molecules signifies the number of detectable photons, which has a direct impact on the localization precision. However, the contrast ratio directly affects the localization precision, primarily by contributing to the background signal. Conversely, the photostability of the molecules under continuous light irradiation is the most important factor from a photochemical point of view, which influences the quality of the images. Hence, it is important to comprehend these photophysical as well as photochemical factors in detail to understand the background for choosing ideal fluorophores for STORM.

3.1. Brightness

The exact position of a single isolated fluorophore can be worth identifying if the centroid of its image could be determined, even if the image spot seems to be diffraction-limited. Though the spatial resolution of a common optical microscope is limited by the width of the point-spread function (PSF), the precise location of a fluorophore can be determined if the image spot of the fluorophore is isolated from the images of other molecules. Therefore, when the precise position of the fluorophore is determined by finding the peak centroid of the image spots, the accuracy can only be influenced by the number of collected photons [12]. Usually, molecular localization coordinates are obtained from statistical curve-fitting algorithms, where the detected photon distribution is fitted to a Gaussian function. Considering fluorescent molecules one by one in the case of negligible background and pixilation, the standard deviation in the fitted position (the uncertainty σ), which actually signifies the precision of the molecular localization can be described using the following equation:

$$\sigma \approx \frac{S}{\sqrt{N}}$$

where S denotes the standard deviation of a Gaussian function representing the point-spread function (PSF) and N is the number of detected photons from the fluorescent probe.

In STORM imaging, it is crucial to minimize the background if a high-precision image with precise molecular localization is anticipated. According to Eq. (1), the resolution of the image can be effectively enhanced by choosing a proper fluorophore with a high brightness. However, for a specific fluorogenic system, the brightness is dependent on two key factors: (a) the extinction coefficient and (b) the fluorescence quantum yield. The extinction coefficient represents how effectively a substance can absorb light at a particular wavelength, so that a fluorophore with a larger extinction coefficient means that it would absorb more photons. The fluorescence quantum yield of a fluorescent probe refers to the ratio of the number of photons emitted to the number of absorbed photons [30]. Therefore, for a given number of absorbed photons, a molecule that possesses a higher quantum yield will have more "brightness". "Photon output" is another term described by Zhuang and coworkers [31] which can provide an idea of the brightness of a given fluorophore. However, it should be kept in mind that other variables, such as drift and labelling density, also contribute significantly to determining the optical resolution of the STORM reconstruction.

3.2. Duty cycle and contrast ratio

As discussed earlier, the most important criterion for obtaining a high-resolution image is to minimize the background signal. In STORM based imaging setup, the background can come up due to the auto-fluorescence of the used reagents or from the used fluorophores. For instance, a photo-switchable fluorophore is expected to switch between the fluorescent "on" and "off" states, where ideally the fluorophore should not have any photon output in the "off" state. However, in reality, the fluorescent "off" state does not usually imply zero photon output. For example, despite being unable to display any meaningful emission profiles, fluorescent probes in a triplet state can still emit weakly and contribute to the background. Therefore, the chosen organic dyes for STORM should emit photons as little as possible in the "off" state and must possess a high contrast ratio.

The duty cycle is another parameter that needs to be investigated when selecting probes for STORM imaging. Upon excitation, at a particular wavelength, a fluorophore emits fluorescence, which is defined as the fluorescence "on" state, whereas the non-emissive state is marked as the "off" state. The duty cycle is basically defined as the ratio of the time a fluorophore spends in the "on" state to that in the "off" state [17]. Hence, a fluorescent molecule having high duty cycle stays in the fluorescence "on" state for a longer period of time, whereas a low-duty cycle molecule spends a very short time in the "on" state and resides most of the time in the "off" state. It should be highlighted that the spatial and temporal separation of the emission outputs are the key factors which need to be closely examined for reconstructing the position of single fluorescence molecules. However, difficulty in accurately identifying a single emitter may arise if the emission profiles substantially overlap with each other. High duty cycle fluorescent probes often encounter the mentioned problem of single molecule localization as their emission profiles overlap significantly. Therefore, fluorophores with a low duty cycle are useful in this respect.

3.3. Photostability

The photostability of a fluorophore plays a crucial role in determining the temporal framework as well as the maximum laser intensity to be used for a microscopy experiment. The photostability of a particular probe can be influenced by both its inherent physicochemical properties, such as switching cycle and survival fraction, as well as the external environment, including pH, temperature and aerial oxidation.

The 'switching cycle' basically refers to the number of cycles a fluorophore switches between its fluorescent "on" and "off" states until it becomes permanently non-fluorescent because of photobleaching. Fluorophores that cannot undergo more than a single switching cycle are not eligible for STORM imaging. Only fluorophores that can switch for hundreds or thousands of cycles are ideal choices for STORM. Although switching cycles differ from fluorophore to fluorophore, the number of cycles is not constant for a particular fluorophore and may vary significantly with changing experimental conditions. Moreover, even though fluorophores with a larger number of 'switching cycles' are preferred in STORM, they might not be suitable for every SMLM imaging application. For instance, a probe with a sole 'switching cycle' is indispensable for quantitative analysis, especially where a 1:1 stoichiometry between the probe and the target is anticipated. On the contrary, while resolving high-resolution fine structures like cytoskeletal

assemblies and biological membrane organization, a greater number of switching cycles are preferable. The desired number of 'switching cycles' will vary depending on the requirements of the information.

It is important to note that dyes having a single switching cycle may encounter localization issues for several potential reasons, such as overlapping with other fluorophore molecules, photobleaching and others. In spite of having a large number of switching cycles, in some cases, the fluorophores can fail to contribute to a high-quality image, as they fade away quickly. For an illumination with specific time (e.g. 400 s), the ratio between the switchable fluorophores in an ensemble compared to that of the fully photo-bleached fluorophores is termed as the 'survival fraction'. This number can be broadly correlated with the average number of potential switching cycles of a particular fluorophore. For example, fluorophores may be photobleached forever without remaining in a weakly emissive state if high-intensity illumination, as in the case of typical STORM techniques, is being used.

4. Photo-switching/photo-blinking: a key feature of fluorescent probes in STORM

Suitable small molecule-based synthetic organic dyes that have been widely used in STORM belong to diverse structural families. A literature survey indicates that cyanine and rhodamine derivatives (Scheme 2) are overwhelmingly used in STORM. A few oxazines and other organic dyes have also been reported from time to time. However, it is worth mentioning that STORM dyes with red-shifted emission/excitation are always preferred more than their blue-shifted counterparts because they have less photo-damaging effects on living cells. Three commonly used dyes, with rhodamine/xanthene (**1**), cyanine (**2**), and oxazine (**3**) cores, are presented in Scheme 2.

A xanthene core (**1**) constitutes the common basic component of many synthetic dyes, such as fluorescein, eosin and rhodamine dyes, which are extensively used in several fluorescence microscopies. As a result, these dyes share many common photophysical properties, even though there are differences in their attached functional groups.

Cyanine (**2**) dyes are the other major class of organic dyes that is often used for STORM imaging. In classic cyanine dyes, there are two nitrogen-containing heterocycles (one is positively charged and the other is charge neutral), which are conjugated to each other through a polymethine chain (—CH groups with alternative single and double bonds) having an odd number of carbon atoms [32,33]. However, in modified cyanines or hemicyanines, a polymethine bridge may be connected to the nitrogen-containing functional groups on either side of the bridge, which constitutes a donor-π-acceptor system [34–36]. Extended π-conjugation in cyanine dyes facilitates the delocalization of energy from absorbed photons to stabilize the electronic transition and hence results in an absorption at a longer wavelength (lower energy) region (Table 1).

As shown in Table 1, the absorption and emission maxima of Cy5 and Cy7 are in the NIR region, which makes them ideal candidates for live cell imaging purposes, as NIR light exerts a less photo-damaging effect, minimum fluorescence background signal and less light scattering outcome compared with UV and visible light irradiation [37–43].

Oxazine (**3**) is another structural family that has been extensively used in various bio-imaging applications. In particular, photoactivatable oxazine fluorophores have been utilized in super-resolution microscopy because of their suitable photo-physical characteristics [44,45].

Table 1
Shift in the absorption and emission of cyanine fluorophores to the longer wavelength region with increasing polymethine chains.

	Polymethine Chain	λ_{abs} (nm)	λ_{em} (nm)
Cy3	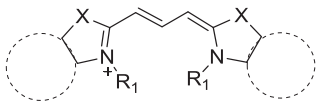	550	562
Cy5	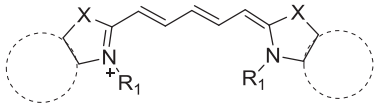	649	664
Cy7	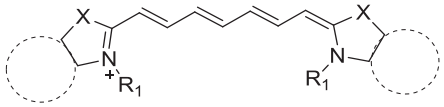	743	774

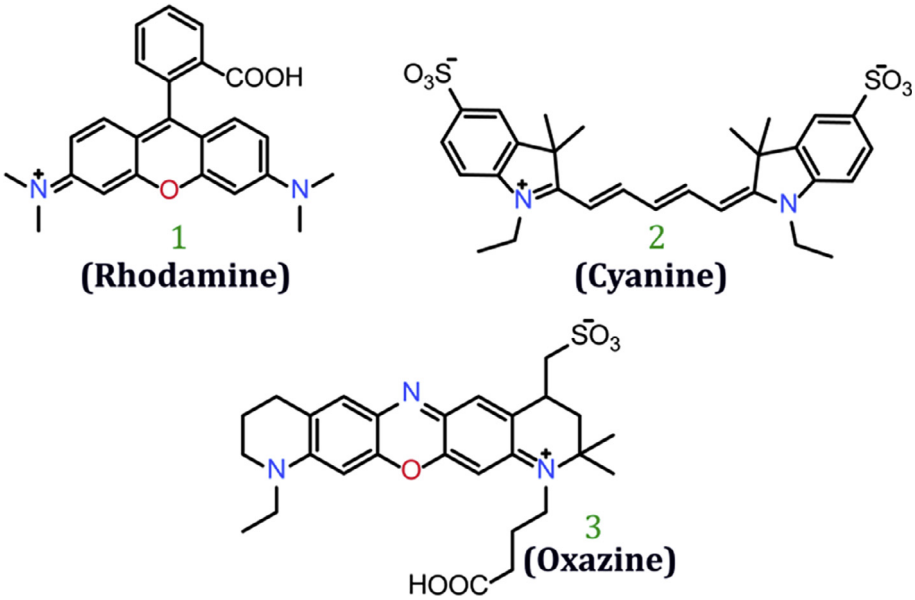

Scheme 2. Structures of fluorophores commonly used in STORM (from the xanthene [**1**], cyanine [**2**], and oxazine [**3**] families).

Controlling the photophysical behavior of fluorophores is essential for achieving good quality successful imaging in every super-resolution microscopy technique. The chosen fluorophores need to exhibit at least two stable and selectively distinguishable states, including fluorescent and dark states, to be utilized in STORM. Moreover, the fluorophores should transition from one state to another with irradiation of light and must spend a suitable period of time in each state to provide useful information (discussed in detail in later sections). It should be noted that the photo-switching processes can either be a reversible transition between a fluorescent and dark state (for example *cis-trans* isomerization), or irreversible transformations like the photo-cleavage of a molecule [16]. Fig. 2 shows a model schematic representation of these photo-switching processes, wherein the photo-switching of a Cy5 dye in the presence of thiols is presented as an example.

In some cases, the photophysics of the fluorophores depends on the occupancy and transition rates between two reversible states. However, in many other cases, more than two states need to be considered to understand the multi-state switching behavior. As summarized in Fig. 2, electronic transitions in normal fluorescence occur from an excited singlet state, and the characteristic lifetime is in the nanosecond range. However, upon spin conversion, the triplet state can be occupied, where the electron excitation can typically last for several microseconds before returning to the ground state. The fluorescence emission of a fluorophore can be considered a constant fluorescence signal as the fluorophore is cycled between the ground and first singlet excited state. However, it can be interrupted occasionally if the electron goes to the triplet state through intersystem crossing (ISC), and this process may continue until the fluorophore is completely photobleached. Fig. 2A illustrates a model photo-switching process, and simply by plotting the photon count over time, normal fluorescence can be distinguished from photo-blinking or photo-bleaching processes, as depicted in Fig. 2B. It should be noted that the typical temporal resolution of an electron multiplying charge coupled device (EMCCD) cameras for super-resolution acquisition is in the millisecond range. Therefore, transitions that are very rapid in nature cannot be distinguished in the accumulated fluorescence emission images. Fast dynamic techniques like fluorescence correlation spectroscopy (FCS) or fluorescence lifetime imaging (FLIM) can be applied in these cases.

However, in other imaging techniques, the dark state might be composed of a highly occupied electronic ground state. For example, in STED, the fluorophore molecules are forcefully sent back to the ground state using a stimulated emission before fluorescence emission can occur. If the molecules are reduced into a semi-radical state or a fully reduced leuco form, then they can only survive up to several minutes or several hours, depending on the chosen environment, as depicted in Fig. 2 [46–49].

Fluorophores can also be kept primarily in the dark state using some caged systems, wherein a photo-reactive group is employed to quench the fluorescence until it undergoes UV light-triggered cleavage of the cage [50]. Endogenous fluorescent proteins can remain in the dark state through several intra-cellular processes. For instance, photo-activation of the final maturation process of a prior uncompleted chromophore, photo-cleavage of the chromophore, or intramolecular dynamics, like a *cis-trans* conformational change, can help these proteins stay in the dark state. Moreover, irreversibly transformable fluorophores can be subjected to reversible blinking with the help of imaging buffers, which eventually can take the fluorescent proteins into reversible dark states, similar to the switching of organic fluorophores.

Ideally, in a photo-switching process, a fluorophore switches between a fluorescent state (denoted $\boldsymbol{F_{on}}$) and a dark state (denoted $\boldsymbol{F_{off}}$), as depicted in the representative model shown in Fig. 3. To enable single-molecule signal detection, the majority of the fluorophores in STORM imaging need to remain in the dark state, so that the rate of $\boldsymbol{k_{off}}$ becomes much higher than the recovering rate $\boldsymbol{k_{on}}$.

By using chemical additives in a special imaging buffer or by applying special mounting media, the switching behavior of most organic dyes can be tuned before employing them in STORM, dSTORM and GSDIM (ground state depletion microscopy). Therefore, the photophysical properties of the fluorophores can be greatly influenced by the strong defining environments, which may alter the state occupancies as well as the transition rates. A list of buffers used in fixed-cell and live-cell STORM imaging is presented in Table 2. It can be mentioned here that photo-switching of the commonly used cyanine dyes in STORM (like Cy5) can be achieved using imaging buffers with variety of thiol concentrations. However, from a toxicity point of view, imaging buffers with low concentrations of the thiol are much more suitable for live cell STORM imaging.

As discussed earlier, molecular oxygen not only acts as a common source for photo-bleaching but also behaves as an efficient triplet state quencher to yield higher fluorescence count rates [51]. Alternatively, this role can be assumed by triplet-state quenchers upon depleting the oxygen with an enzymatic or oxygen scavenger system. However, molecules in excited states can undergo both

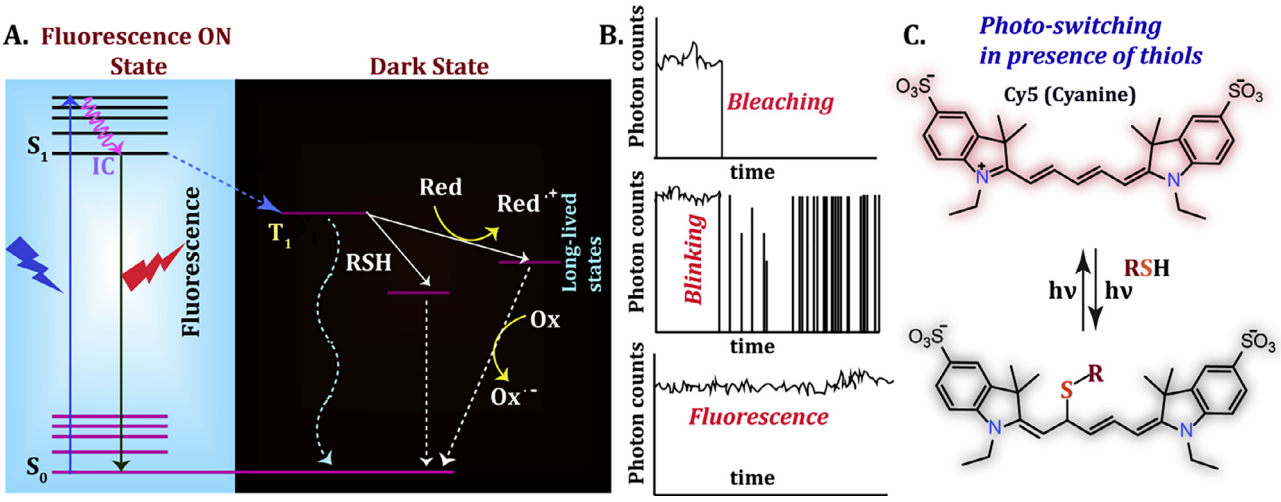

Fig. 2. (A) Schematic representation of photo-switching showing electronic changes through photochemical processes; (B) comparison between normal fluorescence, photo-blinking and photo-bleaching in terms of the photon count over time; and (C) thiol-triggered photo-switching of Cy5 dye.

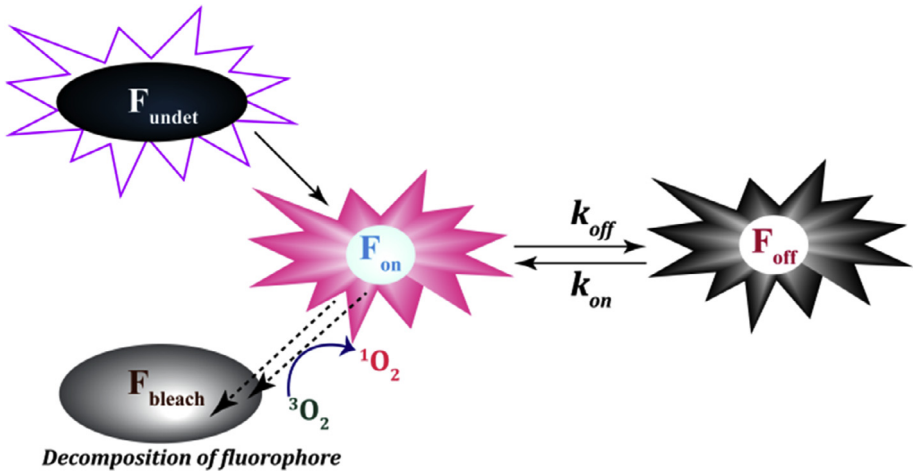

Fig. 3. Exemplary photo-switching model of a fluorophore.

Table 2
Imaging buffers for STORM.

Imaging buffers	Components		
	Buffer solution	Oxygen-scavenging system	Reducing agent
Fixed cell imaging			
MEA/OS 1	Tris (pH 8) + NaCl + glucose	GLOX or POC	MEA
MEA/OS 2	Tris (pH 8) + NaCl	PCD	MEA
BME/OS 1	Tris (pH 8) + NaCl + glucose	GLOX or POC	BME
BME/OS 2	Tris (pH 8) + NaCl	PCD	BME
TCEP	Tris (pH 9) + glucose	GLOX	TCEP and AA
Glycerol/OS	PBS + glucose	GLOX	–
OxEA	PBS (pH = 8–8.5) + Sodium DL-lactate	OxyFluor	MEA
Live cell imaging			
Live-OS 1	L-15 Medium + glucose	GLOX or POC	MEA (Optional)
Live-OS 2	L-15 Medium + glucose	GLOX or POC	BME (Optional)
Live-OS + AA	L-15 Medium + glucose	GLOX or POC	BME (Optional) and AA

Notes: **GLOX:** glucose oxidase and catalase, **POC:** pyranose oxidase and catalase, **PCD:** protocatechuate 3,4-dioxygenase, **MEA:** mercaptoethylamine, **BME:** β-mercaptoethanol, **TCEP:** tris(2-carboxyethyl)phosphine, **AA:** ascorbic acid, **L-15 Medium**: A special medium that supports cell growth in a carbon dioxide (CO_2) free system.

oxidation and reduction. The lower oxidation potential of the triplet state compared with that of the ground state can be attributed to the facile removal of the energy-rich electron from the triplet excited state. Hence, the highest occupied molecular orbital becomes singly occupied, which in turn increases the electron affinity. Subsequently, the collisions of a fluorophore with electron donors or acceptors in the excited state may eventually lead to reduction or oxidation to generate radicals. Some of the molecules that can be successfully utilized as triplet-state quenchers and reductants include glutathione (GSH), dithiothreitol (DTT), β-mercaptoethanol (BME), mercaptoethylamine (MEA), 6-hydroxy-2,5,7,8-tetramethylchroman-2-carboxylic acid (Trolox), cyclooctatetraene (COT) and potassium iodide (KI) [46,52–57]. Additionally, some antioxidants, such as *n*-propyl gallate (*n*PG) or ascorbic acid (AA) [53,58,59], are also used occasionally in STORM imaging. Various other anti-fading reagents often employed to minimize photobleaching include nitrobenzylalcohol (NBA), 1,4-diazabicyclo[2.2.2]octane (DABCO), paraphenylenediamine (PPD) and commercially available products such as Vectashield, Fluorstop, Mowiol, Slow-fade or Citifluor [60–62].

It should be mentioned that various photo-blinking mechanisms have been adopted by several researchers to achieve successful STORM imaging, including (a) a triplet quencher mechanism [48,63], (b) photochromic blinking [64–70], (c) redox blinking [71,72] and (d) other strategies for blinking [73–82].

5. Application of organic dyes for STORM

STORM, in spite of being a relatively new super-resolution microscopy technique (first reported in 2006), has sparked huge interest in chemical biology because of its wide range of applications in bio-imaging to achieve sub-diffraction-limited resolution using fluorescently labelled samples. The localization of fluorescent probes within a sample with photo-switching credentials is the key to procuring a successful STORM image. In addition to providing outstanding resolution (approximately 20 nm lateral resolutions), STORM imaging offers the flexibility of choosing fluorescent dyes and use of aqueous environments, which are essential for live cell imaging. In this section, we will summarize the chronological evolution of STORM imaging in light of the advancement in designing suitable fluorescent probes.

A close look at Schemes 3 and 4 will be helpful for understanding the characteristics of various organic fluorophores that have been used extensively in STORM imaging. Scheme 3 includes the reported fluorophores with blue/green emissions, whereas Scheme 4 represents fluorophores with red/far red/NIR emissions. The fluorophores included in Schemes 3 and 4 have been essentially discussed in this review in the context of various reports. Other fluorophores that are not covered in Schemes 3 and 4 have been discussed separately with structural illustrations in the context of the particular references.

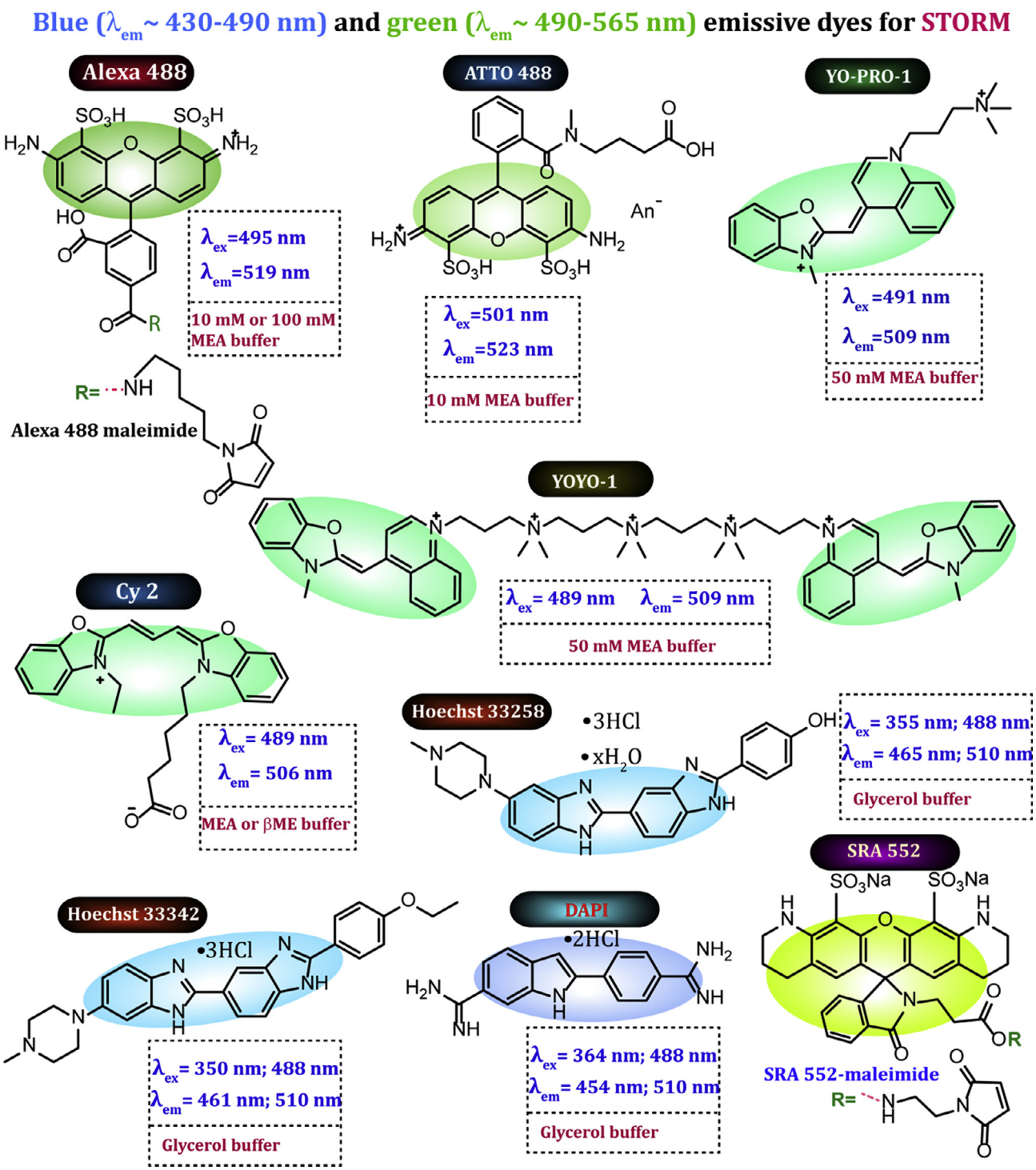

Scheme 3. Structure and properties of blue and green emissive dyes for STORM imaging.

5.1. Multicolor STORM/dSTORM

Multicolor imaging is an important aspect of fluorescence optical imaging that is often used to obtain key biological information. Because biological systems are very complex and dynamic in nature, simultaneous monitoring of the interactions between multiple proteins or cells within an organism using a single color channel is difficult. In this respect, multicolor imaging can serve as a powerful tool to screen different parts of an organ simultaneously and help to understand its functions. For example, Hoffman et al. introduced multicolor cell imaging using fluorescent proteins to track cancer cells and also utilized it to investigate cell-cell interactions on a sub-cellular level [83–85]. However, the use of organic probes for multicolor STORM/d-STORM was achieved much later.

In spite of having tremendous potential to detect molecular interactions via multicolor imaging techniques, fluorescence resonance energy transfer (FRET) [86–89] based imaging lacks the ability to highlight the precise locations and organizations of molecules in subcellular organelles. Fluorescence co-localization

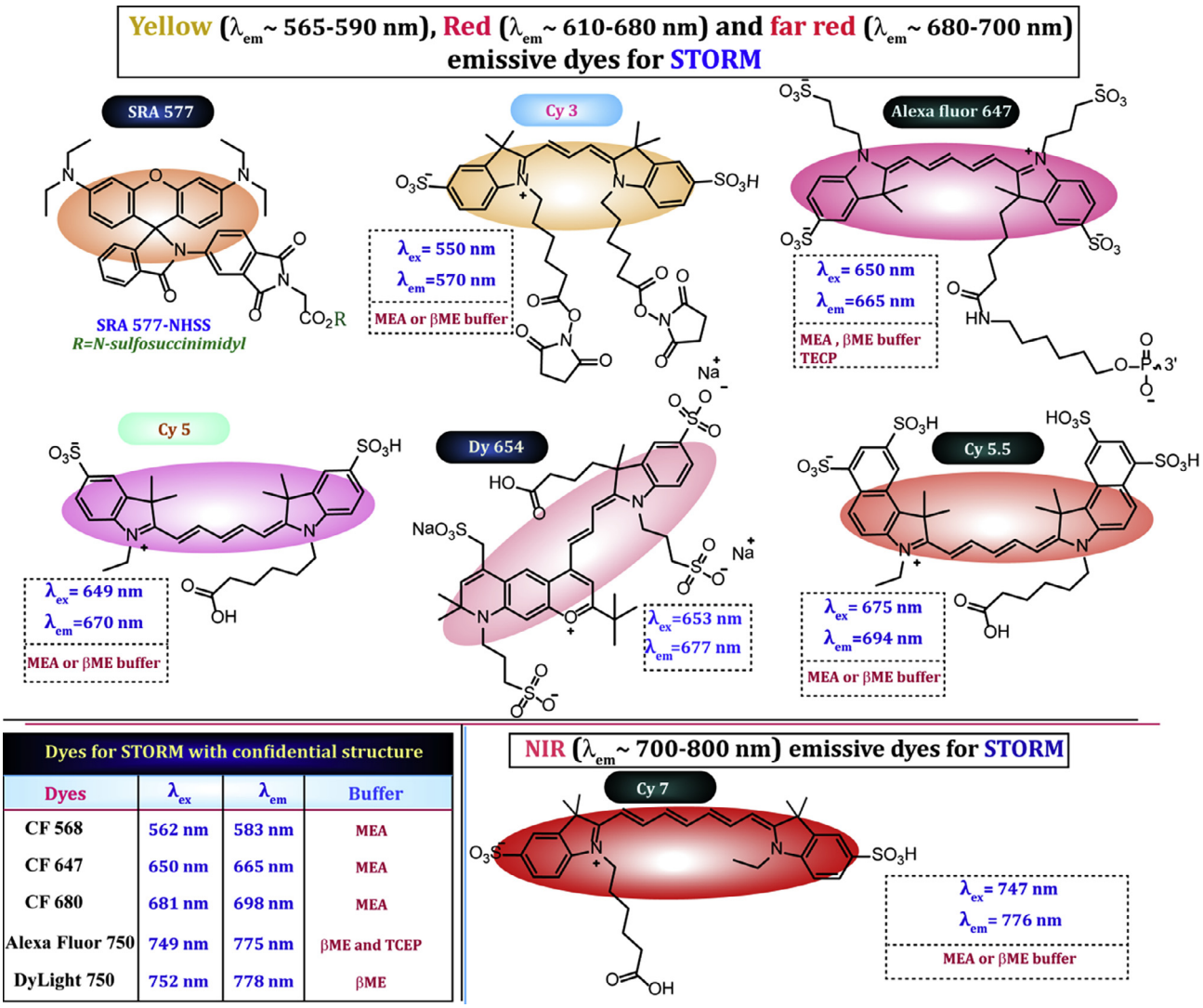

Dyes for STORM with confidential structure

Dyes	λ_{ex}	λ_{em}	Buffer
CF 568	562 nm	583 nm	MEA
CF 647	650 nm	665 nm	MEA
CF 680	681 nm	698 nm	MEA
Alexa Fluor 750	749 nm	775 nm	βME and TCEP
DyLight 750	752 nm	778 nm	βME

Scheme 4. Structure and properties of yellow, red, far-red and NIR emissive dyes for STORM imaging. Note: Some dyes have been presented in the NHS ester (Succinimidyl ester) form.

also faces difficulties in the acquisition of high-resolution multicolor images, as it suffers from the diffraction limit. Combining multicolor imaging with super-resolution techniques can effectively resolve this issue [90].

Zhuang's group was the first to achieve multicolor STORM imaging with 20–30 nm resolution using a reporter-activator pair that belongs to a family of photo-switchable probes with distinct colors [91]. Basically, the Cy2-Alexa 647 dye pair was used for imaging microtubules and the Cy3-Alexa 647 dye pair was used for clathrin imaging. However, for both of the two-color channels, the resolutions were found to be slightly larger (30 ± 1 nm) than that of the resolution determined for single-color STORM images. As expected, the filamentous structures of the microtubules were demonstrated by the green channel, whereas the red channel largely revealed a spherical structure representing clathrin-coated pits. Later in 2008, they developed a multicolor probe where a photo-switchable cyanine dye was linked covalently with an activator molecule [92]. The probe was then employed to monitor the dynamic morphology of mitochondria in a living cell (Fig. 4).

Later, Zhuang and co-workers also screened 26 organic dyes to identify suitable fluorophores for four-color STORM imaging [31]. They found that some of the dyes among all the tested dyes, such as ATTO 488 (blue), Cy3B (orange), Cy5 (red), Dyomics 654 (red), Alexa Fluor 647 (red), DyLight 750 (NIR), Cy7 (NIR) and Alexa Fluor 750 (NIR), which belongs to four distinct spectral ranges, could be satisfactorily used for four-color STORM imaging. In particular, the performances of red dyes like Alexa Fluor 647, Cy5 and Dyomics 654 were found to be remarkably suitable for STORM imaging [31]. It is worth mentioning here that several positively charged cyanine-based dyes, like Alexa Fluor 647, which can exhibit very good performances in STORM imaging, might face several issues when used in live cell imaging purposes. This is because these dyes often encounter cell permeability issues, even though they work fine in fixed cells.

Even though the multi-parameter detection method for multicolor STORM imaging was proposed by Zhuang's group [91] in 2007, it could not be realized experimentally until 2012. Two-color STORM images with multiple emission channels were obtained by them [93] using Alexa 750 in conjunction with Alexa 647, wherein the use of two or more fluorescence detection channels for STORM provided the scope to obtain multicolor images with reduced color crosstalk.

A common strategy for separating the signal is often used in multicolor STED [90], PALMIRA [94], STORM [91] and PALM [95]

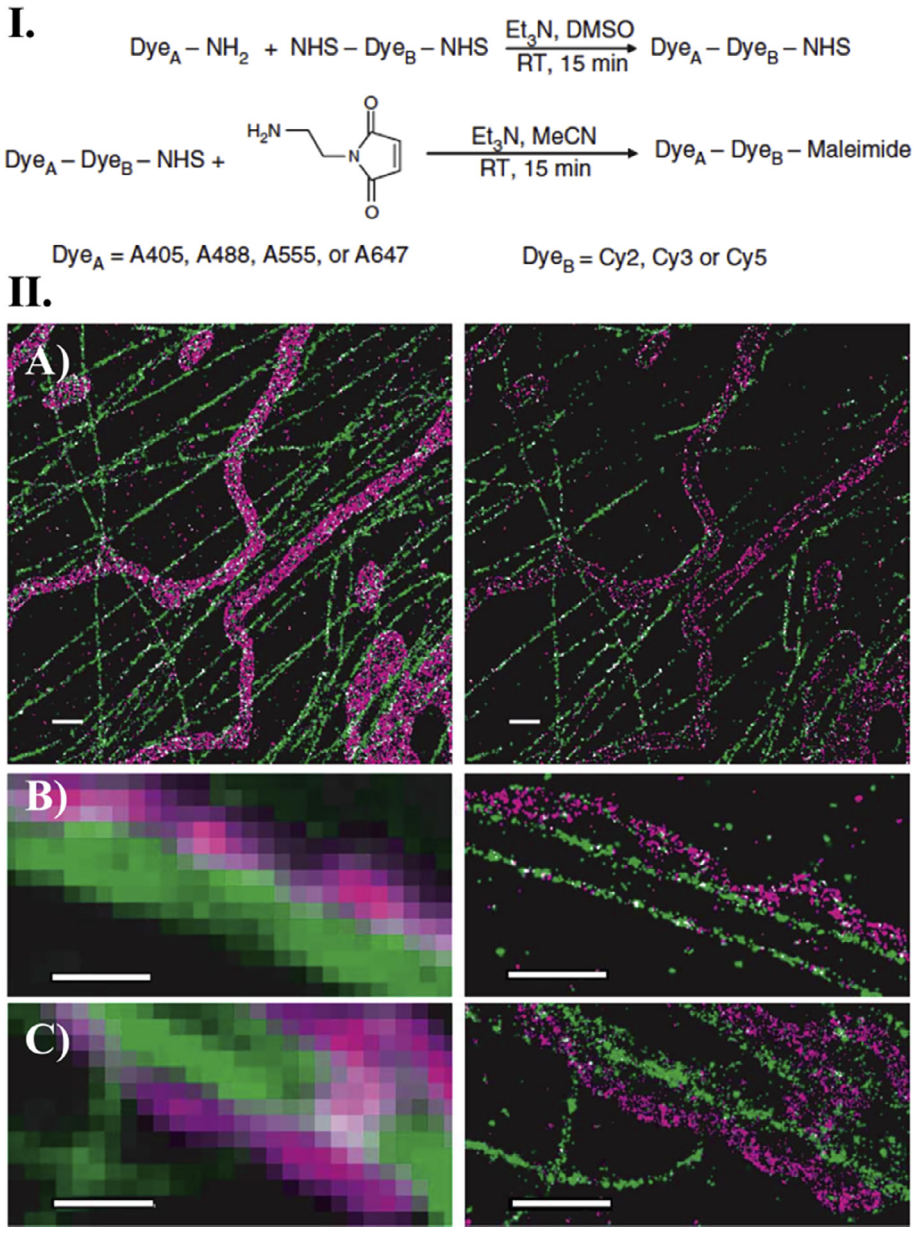

Fig. 4. I. Synthetic scheme for a covalently linked photo-switchable activator-reporter pair; II. Two-color STORM images, in comparison with conventional fluorescence images, showing the interactions between tubular mitochondria (magenta) and microtubules (green) in three BS-C-1 cells. Adapted from Zhuang et al. [92] with the permission of Nature and its sister journal publishing group.

imaging, wherein specific excitation wavelengths are selected for different markers, followed by the careful selection of emission filters to minimize the crosstalk between the different color channels. However, the lack of flexibility in choosing the fluorescent dyes and the source of light makes this approach unattractive. To deal with these issues, Schonle and Hell [96] adopted a new approach in place of the conventional sequential multicolor separation approach, wherein up to three different switchable rhodamine amides were simultaneously used to achieve single-molecule switching-based nanoscale imaging, depending on the individual characteristic emission spectra (Fig. 5). The new approach not only provided the scope for simultaneous multicolor imaging with low crosstalk, but also yielded an impressive spatial resolution of 15 nm. Hence, the strategy was later adopted for cell imaging purposes. With the help of this strategy, the microtubule and keratin network of mammalian cells has been successfully identified using SRA577 and SRA552 dyes. Later, other rhodamine spiroamides were also developed by Belov and Hell [97] for multicolor super-resolution imaging. However, the photo-physical properties of these rhodamine spiroamides are vulnerable to a change in the pH value of the experimental conditions. So, this aspect should be looked into before employing them in a STORM imaging experiment.

Heileman and Sauer later developed a new method for STORM imaging, termed direct STORM (dSTORM), to avoid the use of dye-pairs. In the dSTORM approach, conventional cyanine dyes (Cy5, Alexa 647) can be directly used for cellular staining, so no additional activator fluorophore is required [98]. This approach was then applied by the same group for multicolor imaging [99]. Essentially, standard fluorophores with different absorption and emission wavelengths, such as ATTO520 and ATTO655, were employed to obtain multicolor d-STORM imaging of microtubule filaments and enzymes of the respiratory chain with the highest optical resolution of ~20 nm.

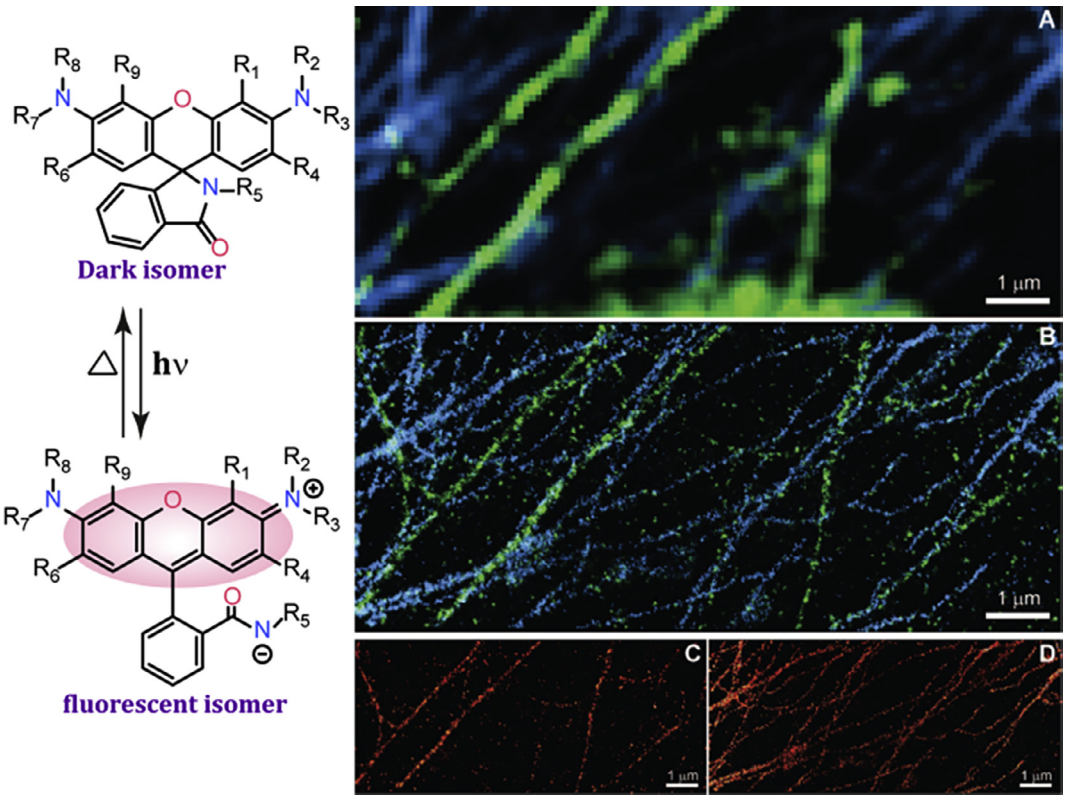

Fig. 5. Left: plausible switching mechanism between the fluorescent and dark states of rhodamine amides; Right: Classical wide-field image and nanoscopy image of the microtubule and keratin network immunostained with SRA552-maleimide (blue) and SRA577-NHSS (green). Adapted from Hell et al. [96] with the permission of the American Chemical Society.

Multicolor super-resolution imaging is vulnerable to channel crosstalk and registration errors, which curb its application potential. To overcome these common limitations, a novel variant of dSTORM has been reported by Schmoranzer and co-workers [100], defined as spectral demixing dSTORM (SD-dSTORM). Basically, combining the principle of spectral demixing and the diverse photophysical properties of red-emitting carbocyanine dyes ultimately results in efficient, reliable and fast multicolor dSTORM imaging. Later, Lehmann and Schmoranzer [101] screened a total of 39 dyes to identify novel dyes that are suitable for multicolor caged dSTORM using this method. A multicolor localization precision as low as 15 nm has been achieved using a dye pair suitable for registration error-free multicolor SD-dSTORM. Further, using the caged SD-dSTORM, they were able to resolve the ultrastructure of single synaptic vesicles in brain sections (maximum resolution 40 nm) with improved label density in two independent channels compared with that of immuno-electron microscopy (Fig. 6) [101].

Later, they studied 28 commercially available dyes and reported [102] that the spectroscopic properties of the dye pair CF647 and CF680 are suitable for achieving registration error-free dual-color SD-dSTORM with minimal color crosstalk (discussed in detail later).

5.2. 3D STORM

Expansion of STORM imaging to a third dimension has introduced a tectonic shift in the technical advancement of STORM imaging. There were difficulties in obtaining accurate information concerning the axial position of a fluorophore when focused in a single 2D plane, as the speed of the on-off switching in 2D-STORM precluded the acquisition of a z stack during any single emission event. On the contrary, 3D STORM allows the 3D imaging of a sample with a thickness of several hundred nanometers without any scanning. However, with an increase in the thickness of the sample, the image of a molecule becomes more blurred, which ultimately limits the overall localization precision.

Zhuang's group was the first to achieve a 3D STORM image [103]. They used 3D STORM to resolve the 3D morphology of nanoscopic structures in cells. Essentially, clathrin-coated pits (CCPs), which have spherical cage-like structures (150–200 nm in size), were successfully imaged through a direct immunofluorescence scheme using primary antibodies against clathrin doubly labelled with Cy3 and Alexa 647 [103]. In addition to achieving the 3D super-resolution imaging of CCPs in fixed cells [103], they have also obtained 3D super-resolution images of CCPs in live cells [104] and in the entire mitochondrial network [31,92]. However, precisely determining the axial positions remains the main challenge for localization precision in STORM, as it depends on the number of photons detected from each fluorophore. Even the interferometric detection method, which generally provides the most precise z-localization, often encounters the same issue [105,106]. Hence, to resolve this issue, a new approach was adopted by Zhuang's group [107], wherein the resolution of the image could be increased by combining 3D STORM with a complex optical setup. The complex optical setup actually included two opposing lenses to double the photon collection. They were able to achieve STORM images with a resolution of <10 nm in the lateral direction and <20 nm in the axial direction using Alexa 647.

Later, Moerner and Piestun [108] introduced another 3D super-resolution approach based on a double-helix point spread function (DH-PSF), which can be utilized for imaging far beyond the diffraction limit (Fig. 7). They were able to achieve super localization of single fluorescent molecules in thick samples with precisions as low as 10 nm laterally and 20 nm axially over axial ranges >2 μm. Basically, a photoactivatable 2-dicyanomethylene-3-cyan

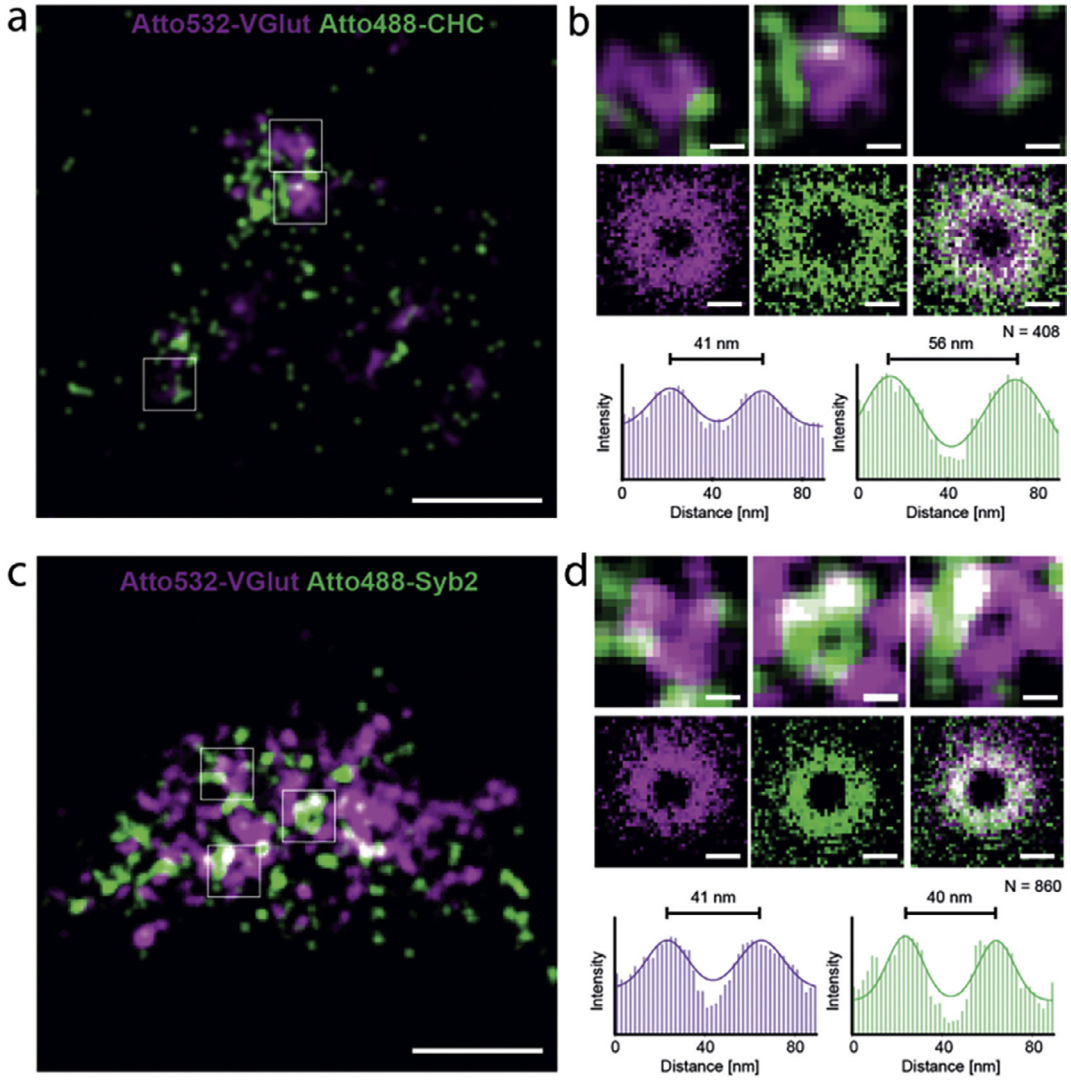

Fig. 6. Presynaptic terminals of mouse brain (150 nm cryosections) immunolabelled for VGlut/clathrin (a, b) and VGlut/Syb2 (c, d) showing caged SD-dSTORM imaging. Adapted from Lehmann et al. [101] with the permission of WILEY-VCH Verlag GmbH & Co. KGaA, Weinheim.

o-2,5-dihydrofuran (DCDHF)-based fluorophore was used for the 3D super-resolution imaging of highly concentrated single molecules in a bulk polymer (Fig. 7).

5.3. Live-cell STORM imaging

In general, it is very difficult to achieve live-cell STORM imaging because a single reconstruction of STORM imaging typically requires thousands of individual frames of image data, making the process too slow to be utilized in real-time live cell monitoring. Still, some reports have demonstrated successful time-resolved live cell STORM imaging of multiple targets with minimal motion-induced blur.

The first live-cell STORM imaging was reported by Heinemann and Sauer's group [46] in 2010, wherein a novel and facile method was introduced to use standard Alexa Fluor and ATTO dyes for live cell super-resolution imaging. Frequently used fluorophores like Alexa Fluor and ATTO dyes can switch reversibly between on and off states under similar experimental conditions in the visible wavelength range. Essentially, the super-resolution imaging of mRNA in A549 cells was successfully achieved using oligo (dT) 43-mer labelled with ATTO655. However, it should be kept in mind that the ATTO655 dye is not readily cell permeable and it often needs to be conjugated with suitable functionality before employing it in a live cell experiment.

Cornish and Sauer also reported a trimethoprim chemical tag (TMP tag) using the same ATTO655 fluorophores, suitable for stochastic single molecule-based localization microscopy (dSTORM method) [109]. They demonstrated that when the human histone H2B protein in live mammalian cells is labelled with TMP-ATTO655, the dSTORM-TMP tag could substantially improve the spatiotemporal resolution in live cells (Fig. 8). However, as they did not characterize the localization density, the image resolution achieved in that 2D super-resolution imaging remained unsatisfactory. In 2011, Zhuang's group used photoswitchable dyes to achieve high spatial and temporal resolutions in 2D- and 3D-STORM super-resolution imaging of live cells [104]. In 2D STORM, they obtained a Nyquist resolution of ~20 nm with a time resolution of 0.5 s, whereas for 3D volumetric super-resolution imaging of live cells, an overall resolution of 30 nm in the x-y dimension and 50 nm in the z dimension was achieved with an impressive time resolution of 1–2 s. Later, the dSTORM imaging of DNA in living cells was achieved by Manley and coworkers using the commercially available cyanine-based Picogreen dye [110]. The

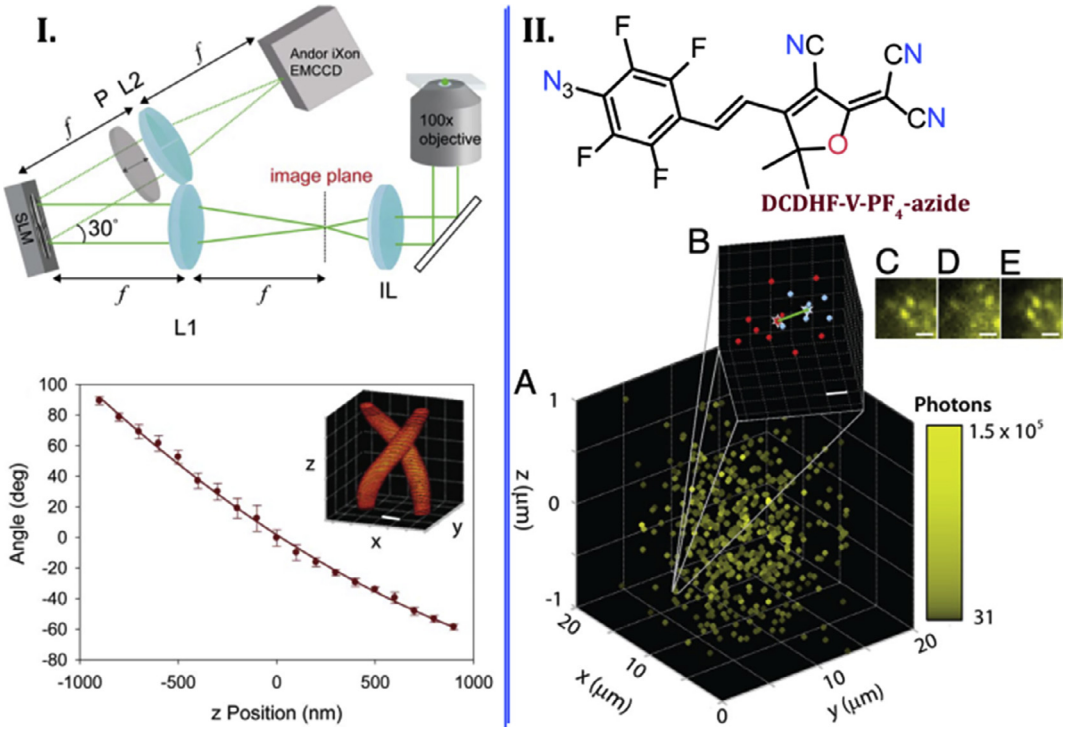

Fig. 7. I. DH-PSF setup for 3D super-resolution imaging and a calibration curve for z-calibration II. Structure of the fluorophore and (A–E) 3D super-resolution imaging with the DH-PSF setup using the PALM/STORM/F-PALM method. Adapted from Moerner et al. [108].

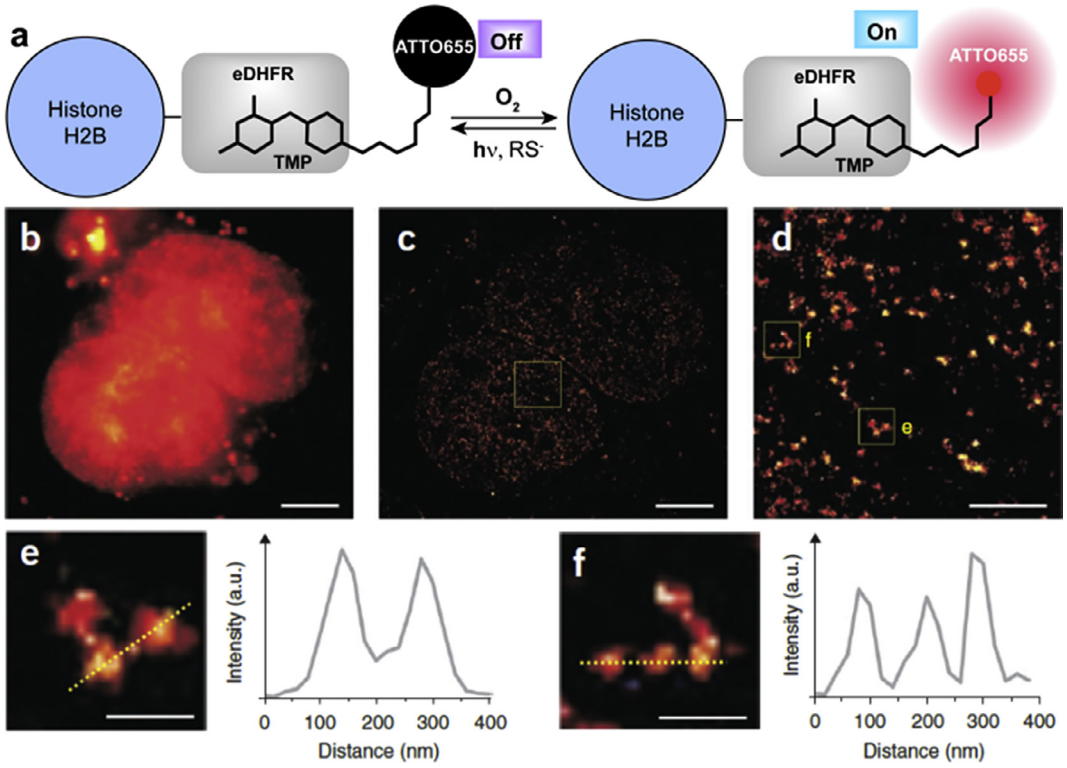

Fig. 8. (a) Schematic representation of the TMP-eDHFR labelling system used for dSTORM. (b) Wide-field fluorescence image of TMP-ATTO655-bound core histone H2B proteins in the nucleus of living HeLa cells; (c) corresponding dSTORM image; (d) an expanded view of the boxed area in c; (e–f) expanded views of the marked regions in d (left) and cross-sectional profiles along the dashed lines. Scale bars, 5 μm (b, c), 1 μm (d), 200 nm (e, f). Reproduced from Sauer et al. [109] with the permission of WILEY-VCH Verlag GmbH & Co. KGaA, Weinheim.

addition of potentially toxic thiol reducing agents such as MEA, which are commonly used to induce photoblinking, was avoided by this research group to ensure the feasibility of live-cell imaging. By studying the buffer conditions of live-cell dSTORM for other dyes, the same research group found that 1 nM ascorbic acid combined with an oxygen scavenger (OS) system in Leibowitz medium at pH 7.2 is optimum for rapid and reversible photo-switching [61,72]. In the same buffer conditions, they obtained successful dSTORM (direct labelling with the commercially available cyanine-based Picogreen dye) imaging of DNA in living cells (discussed in detail later). Again in 2012, Zhuang's group [111] was able to achieve dynamic imaging of specific membrane structures in living cells with a spatial resolution of 30–60 nm and a temporal resolution down to 1–2 s, wherein common membrane probes like carbocyanine dyes with long alkyl chains were used as the fluorophore [111]. In this context, it should be mentioned here that cyanine dyes often lose their applicability in long term live cell STORM imaging in spite of their good photo-physical properties as they need imaging buffers containing thiols to achieve 'photo-switching' which essentially hampers the cell viability. In the recent past (2013), Johnsson and co-workers [112] introduced a new silicon-rhodamine-based near-infrared probe that can be specifically coupled to proteins using various labelling strategies. The biocompatible NIR probe displayed several beneficial attributes, such as good cell permeability, high fluorescence quantum yield and good brightness and photostability, which made it suitable for achieving live-cell super-resolution imaging of proteins in living cells and tissues.

Later, in 2014, a new class of spontaneously blinking fluorophores based on the intramolecular spirocyclization reaction was reported by Urano et al. [113] (Fig. 9). Using the fluorophore (HMSiR) and a spinning-disk confocal microscope, they were able to demonstrate SLM of proteins located far above the coverslip surface. Repetitive time lapse SLM of microtubules in live cells for 1 h was also demonstrated. However, the main drawback of this fluorogenic system is that it only works fine in intra-cellular non-acidic compartments. The probe might not be applicable in most intracellular dysfunctions related studies which produce a lower pH environment.

5.4. Other STORM imaging

In addition to the categorized STORM imaging techniques mentioned above, various other STORM imaging techniques have been achieved that also have made a considerable contribution to the evolution of STORM microscopy. For instance, in 2009, Flors and co-workers [114] noted that commercially available intercalating cyanine dyes, such as YOYO-1, could be readily utilized for labelling and imaging DNA with a single laser to achieve super-resolution imaging. Later, they reported that green intercalating dyes (YO-PRO-1) have good potential for uncovering the nanoscale organization of DNA in both DNA-based nanotechnology and some biological applications [115].

Later, in 2012, Sauer's group [116] was able to study the structure of a nuclear pore complex (NPC) in isolated *Xenopus laevis* oocyte nuclear envelopes using dSTORM. A lateral resolution of ~15 nm was achieved in that experiment.

With the help of STORM, Cordes and co-workers studied the mechanism of intramolecular photo-stabilization in self-healing cyanine dyes, which can repair photo damage automatically [117]. In 2013, Zhuang's group [67] noticed that cyanine fluorophores could be reversibly quenched by the phosphine tris(2-carboxyethyl)phosphine (TCEP). The TCEP-induced photo-reversible quenching subsequently became instrumental in acquiring high-quality super-resolution images as well as an easy-to-implement cellular internalization assay.

Birk and co-workers [118] effectively employed DNA minor groove binding dyes, like Hoechst 33258, Hoechst 33342, and DAPI, in single-molecule localization microscopy to obtain high optical and structural resolution. With a similar approach, the local distri-

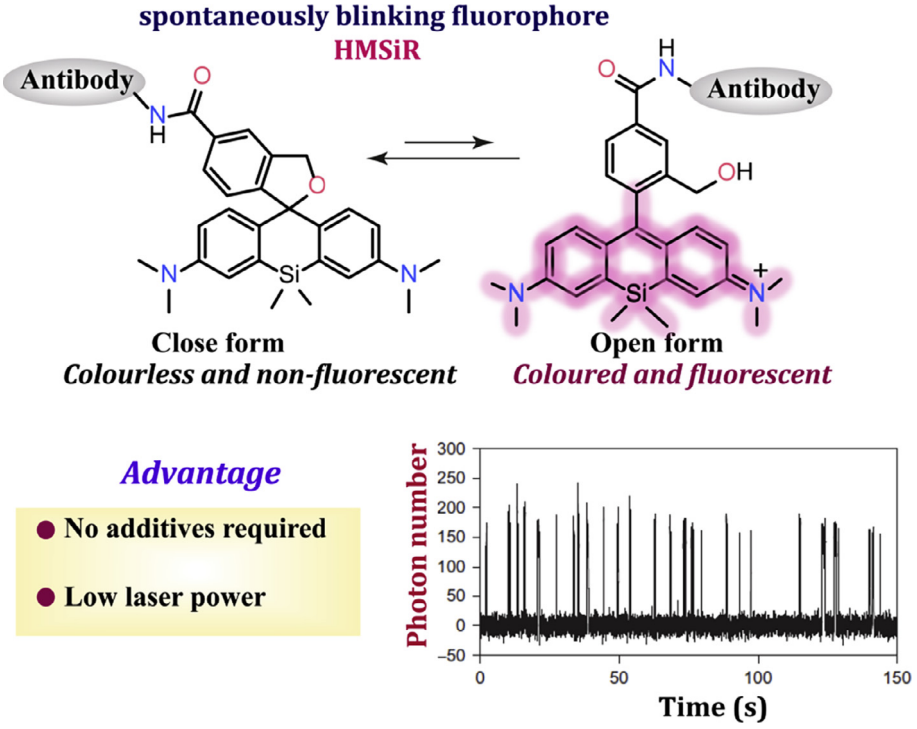

Fig. 9. Switching mechanism of the spontaneously blinking fluorophore HMSiR, showing reversible blinking over a hundred times resulting from intramolecular spirocyclization. Reproduced in parts from Urano et al. [113] with the permission of Nature Chemistry, Macmillan Publishers Limited.

bution of DNA in the cell nucleus and in mitotic chromosomes was studied through optical imaging, which actually improved the resolution to a few tens of nanometers.

As mentioned earlier, Schmoranzer [102] tested as many as 28 commercially available dyes to determine their potential applicability in super-resolved cellular nanostructure determination. Eight among those dyes were identified as suitable fluorescent probes for high-quality dSTORM imaging in various spectral regimes. Dye pairs with similar spectral properties (for instance, CF647 and CF680) are most suitable for spectral demixing-based registration error-free multicolor dSTORM imaging with low crosstalk. The same dye pair and another CF568 dye with different spectral properties were used together to perform 3-color dSTORM, which was instrumental in resolving the nanostructures of the cytoskeleton and the membrane trafficking machinery (Fig. 10).

Recently, Cremer [119] and coworkers revealed that the standard DNA dye Vybrant dye-cycle ™ VIOLET CANBE can be successfully used to achieve single-molecule localization microscopy images of DNA in the nuclei of fixed mammalian cells.

Even though single-molecule localization microscopy (SMLM) is a useful method for constructing super-resolution images, it often requires additives like thiols to induce on-off switching of fluorophores along with intense prior laser irradiation, which adversely affects its application potential. In this context, Urano et al. reported a spontaneously blinking fluorophore, in which the intramolecular spirocyclization reaction was used as the key to achieve spontaneous blinking, as discussed earlier. Recently, in 2017, nacre proteins of the pearl oyster *Pnictada fucata* were successfully labelled with Cy5 by Zhang and co-workers [120]. The distribution of the nacre proteins inside the whole synthetic calcite was then directly observed using STORM imaging.

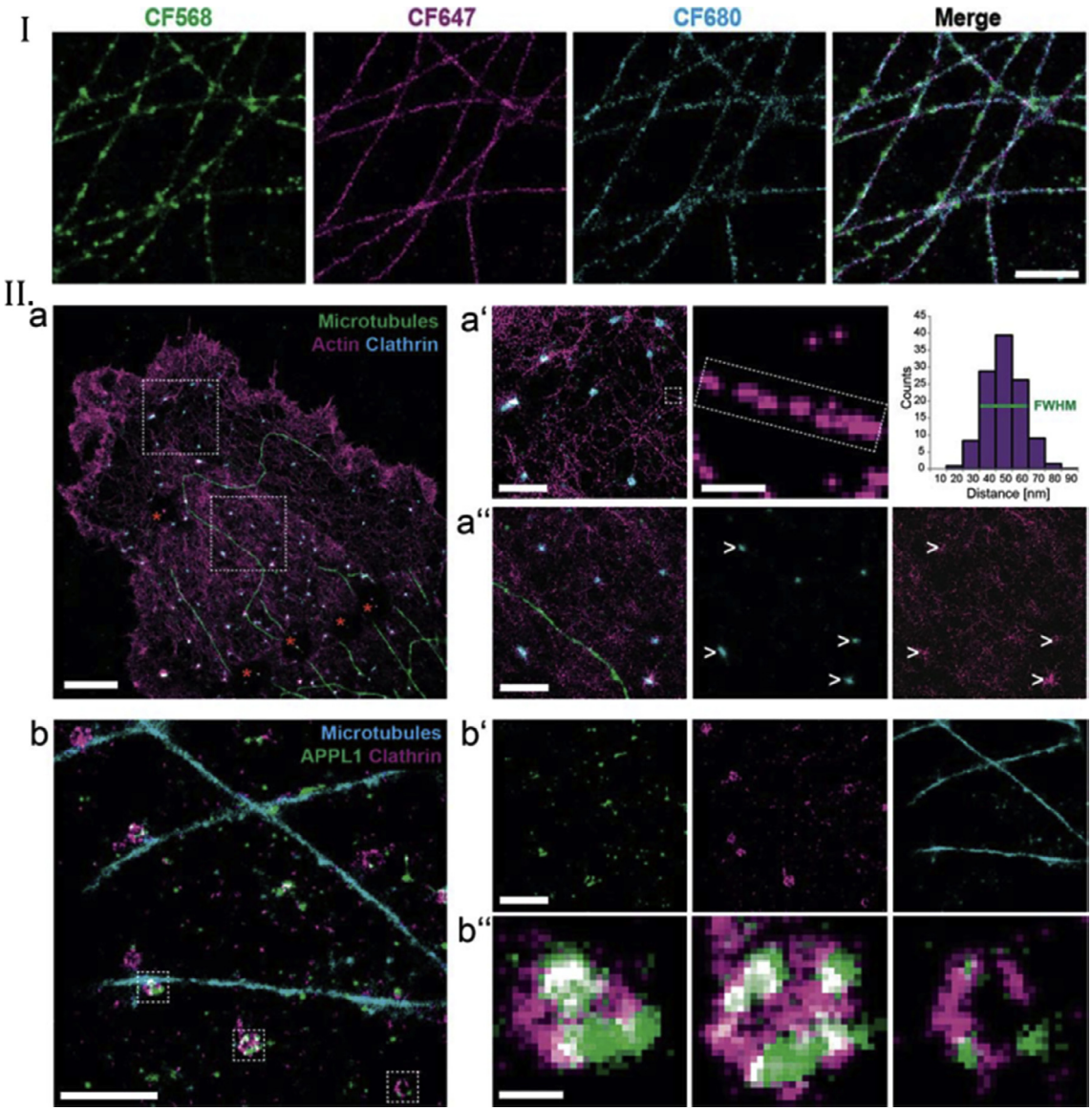

Fig. 10. I. NIH 3T3 cells, co-immunolabelled for MTs with CF647/CF680 and CF568 dyes showing 3-color dSTORM imaging; II. COS-7 cells, immunolabelled for (a) MTs (CF568), f-actin (phalloidin CF647) and clathrin (CF680) and for (b) APPL1 (CF568), clathrin (CF647) and MTs (CF680) to achieve 3-color dSTORM imaging. Reproduced in part from Schmoranzer et al. [102] with the permission of WILEY-VCH Verlag GmbH & Co. KGaA, Weinheim.

6. Conclusion and future perspectives

The STORM approach has been shown to be a very promising tool that provides a new convenient platform to study complex cellular processes with sub-diffraction resolution. This review not only highlights the recent advancements in STORM-based super-resolution imaging applications with the use of organic small molecule fluorescent probes, but also includes a brief discussion about the choice of suitable fluorophores to achieve successful STORM imaging. The essential criteria to design and develop new organic fluorescent probes for STORM have been outlined here with detailed mechanistic insights so that the desired modifications can expedite future progress in probe design. Undoubtedly, the utility of this imaging approach will grow further with the continuing expansion of STORM-based imaging technology as well as new labelling methods in the near future. With the appropriate choice of fluorescent probes, it is possible to visualize dynamic changes in subcellular organelles with sub-diffraction resolution using live cell STORM imaging, which can potentially open a new window for resolving physiological ailments pertaining to cellular dysfunctions. As the choice of suitable fluorophores constitutes the most important element of procuring a good quality successful high-resolution image, there is an on-going endeavor to develop new versatile fluorophores with outstanding features for the improvement of imaging quality. Even though there has been a great deal of advancement in STORM-based imaging with the use of organic fluorescent dyes, there are still many issues that need to be squarely addressed. For instance, in multicolor STORM imaging, the fluorophores can be activated by the "wrong" activation pulse because the fluorophores can become activated spontaneously without any activation pulse. Alternately, if the 'fluorophores pair' strategy is used to counter this problem, it would be free from chromatic aberrations but it might then suffer from color cross-talk. On the contrary, in dSTORM, even though the color cross-talk can be reduced, it is difficult to correct chromatic aberrations at the nanoscale level. Essentially, single-molecule localization-based super-resolution imaging techniques like STORM may suffer huge setbacks if a suitable fluorophore is not chosen. Hence, the development of new fluorophores with improved qualities will become instrumental in pioneering STORM-based high-resolution images. Therefore, the endeavor will continue to design and develop better probes suitable for STORM until the ideal fluorescent probe is developed. The use of efficient organic fluorescent probes in STORM has the potential to be used in medical diagnosis, as it can be utilized to acquire quantitative information about the specific expression profiles in subcellular organelles; hence, this technique can be utilized for personalized therapies. In this respect, we strongly believe this focused review article will contribute tremendously to the development of novel fluorescent probes for advanced imaging, which will boost the active field of research to study subcellular processes with a sub-diffraction limit.

Acknowledgments

This work has been partially supported by the National Natural Science Foundation of China (No. 61525503, 61875131, 21406125, 61620106016, 81727804); the National Basic Research Program of China (No. 2015CB352005); Guangdong Natural Science Foundation Innovation Team (No. 2014A030312008); the Shenzhen Basic Research Project (No. JCYJ20170818100931714, JCYJ20150930104948169, JCYJ20160328144746940, GJHZ20160226202139185, JCYJ20170412105003520) and the National Creative Research Initiative programs of the National Research Foundation of Korea (NRF) funded by the Korean Government (No. 2018R1A3B1052702).

Appendix A. Supplementary data

Supplementary data associated with this article can be found, in the online version, at https://doi.org/10.1016/j.ccr.2018.08.006.

References

[1] S. Kolemen, E.U. Akkaya, Reaction-based BODIPY probes for selective bio-imaging, Coord. Chem. Rev. 354 (2018) 121–134.
[2] K. Kikuchi, Design, synthesis and biological application of chemical probes for bio-imaging, Chem. Soc. Rev. 39 (2010) 2048–2053.
[3] L. Yuan, W.Y. Lin, K.B. Zheng, L.W. He, W.M. Huang, Far-red to near infrared analyte-responsive fluorescent probes based on organic fluorophore platforms for fluorescence imaging, Chem. Soc. Rev. 42 (2013) 622–661.
[4] E. Betzig, J.K. Trautman, Near-field optics – microscopy, spectroscopy and surface modification beyond the diffraction limit, Science 257 (1992) 189–195.
[5] M.G.L. Gustafsson, Surpassing the lateral resolution limit by a factor of two using structured illumination microscopy, J. Microsc. 198 (2000) 82–87.
[6] M.G.L. Gustafsson, Nonlinear structured-illumination microscopy: wide-field fluorescence imaging with theoretically unlimited resolution, PNAS 102 (2005) 13081–13086.
[7] S.W. Hell, J. Wichmann, Breaking the diffraction resolution limit by stimulated-emission – stimulated-emission-depletion fluorescence microscopy, Opt. Lett. 19 (1994) 780–782.
[8] T.A. Klar, S. Jakobs, M. Dyba, A. Egner, S.W. Hell, Fluorescence microscopy with the diffraction resolution barrier broken by stimulated emission, PNAS 97 (2000) 8206–8210.
[9] E. Betzig, G.H. Patterson, R. Sougrat, O.W. Lindwasser, S. Olenych, J.S. Bonifacino, M.W. Davidson, J. Lippincott-Schwartz, H.F. Hess, Imaging intracellular fluorescent proteins at nanometer resolution, Science 313 (2006) 1642–1645.
[10] M.J. Rust, M. Bates, X.W. Zhuang, Sub-diffraction-limit imaging by stochastic optical reconstruction microscopy (STORM), Nat. Methods 3 (2006) 793–795.
[11] S.T. Hess, T.P.K. Girirajan, M.D. Mason, Ultra-high resolution imaging by fluorescence photoactivation localization microscopy, Biophys. J. 91 (2006) 4258–4272.
[12] M. Bates, S.A. Jones, X. Zhuang, Stochastic optical reconstruction microscopy (STORM): a method for superresolution fluorescence imaging, Cold Spring Harb. Protoc. (2013), https://doi.org/10.1101/pdb.top075143.
[13] M. Sauer, M. Heilemann, Single-molecule localization microscopy in eukaryotes, Chem. Rev. 117 (2017) 7478–7509.
[14] M.B. Stone, S.A. Shelby, S.L. Veatch, Super-resolution microscopy: shedding light on the cellular plasma membrane, Chem. Rev. 117 (2017) 7457–7477.
[15] J. Tam, D. Merino, Stochastic optical reconstruction microscopy (STORM) in comparison with stimulated emission depletion (STED) and other imaging methods, J. Neurochem. 135 (2015) 643–658.
[16] E.M.S. Stennett, M.A. Ciuba, M. Levitus, Photophysical processes in single molecule organic fluorescent probes, Chem. Soc. Rev. 43 (2014) 1057–1075.
[17] J.R. Allen, J.S. Silfies, S.A. Schwartz, M.W. Davidson, Single-Molecule Super-Resolution Imaging, https://www.microscopyu.com/techniques/super-resolution/single-molecule-super-resolution-imaging.
[18] Z. Yang, A. Sharma, J. Qi, X. Peng, D.Y. Lee, R. Hu, D. Lin, J. Qu, J.S. Kim, Super-resolution fluorescent materials: an insight into design and bioimaging applications, Chem. Soc. Rev. 45 (2016) 4651–4667.
[19] J. Li, N. Kwon, Y. Jeong, S. Lee, G. Kim, J. Yoon, Aggregation-induced fluorescence probe for monitoring membrane potential changes in mitochondria, ACS Appl. Mater. Interfaces 10 (2018) 12150–12154.
[20] J. Zhao, G.R. Jin, G.J. Weng, J.J. Li, J. Zhu, J.W. Zhao, Recent advances in activatable fluorescence imaging probes for tumor imaging, Drug Discovery Today 22 (2017) 1367–1374.
[21] T. Etrych, H. Lucas, O. Janouskova, P. Chytil, T. Mueller, K. Mader, Fluorescence optical imaging in anticancer drug delivery, J. Controlled Release 226 (2016) 168–181.
[22] W. Stummer, E.S. Molina, Fluorescence imaging/agents in tumor resection, Neurosurg. Clin. N. Am. 28 (2017) 569–583.
[23] D.R. Miller, J.W. Jarrett, A.M. Hassan, A.K. Dunn, Deep tissue imaging with multiphoton fluorescence microscopy, Curr. Opin. Biomed. Eng. 4 (2017) 32–39.
[24] I.R. Correa Jr., Live-cell reporters for fluorescence imaging, Curr. Opin. Chem. Biol. 20 (2014) 36–45.
[25] R.E. Thompson, D.R. Larson, W.W. Webb, Precise nanometer localization analysis for individual fluorescent probes, Biophys. J. 82 (2002) 2775–2783.
[26] G.T. Dempsey, M. Bates, W.E. Kowtoniuk, D.R. Liu, R.Y. Tsien, X. Zhuang, Photoswitching mechanism of cyanine dyes, J. Am. Chem. Soc. 131 (2009) 18192–18193.
[27] J.K. Jaiswal, S.M. Simon, Potentials and pitfalls of fluorescent quantum dots for biological imaging, Trends Cell Biol. 14 (2004) 497–504.
[28] D.M. Shcherbakova, P. Sengupta, J. Lippincott-Schwartz, V.V. Verkhusha, Photocontrollable fluorescent proteins for superresolution imaging, Annu. Rev. Biophys. 43 (2014) 303–329.
[29] V. Adam, R. Berardozzi, M. Byrdin, D. Bourgeois, Phototransformable fluorescent proteins: future challenges, Curr. Opin. Chem. Biol. 20 (2014) 92–102.

[30] J.R. Lakowicz, Principles of Fluorescence Spectroscopy, third ed., Springer, US, Boston, MA, 2006.
[31] G.T. Dempsey, J.C. Vaughan, K.H. Chen, M. Bates, X. Zhuang, Evaluation of fluorophores for optimal performance in localization-based super-resolution imaging, Nat. Methods 8 (2011) 1027–1036.
[32] A. Mishra, R.K. Behera, P.K. Behera, B.K. Mishra, G.B. Behera, Cyanines during the 1990s: a review, Chem. Rev. 100 (2000) 1973–2011.
[33] W. Sun, S. Guo, C. Hu, J. Fan, X. Peng, Recent development of chemosensors based on cyanine platforms, Chem. Rev. 116 (2016) 7768–7817.
[34] S. Samanta, P. Dey, A. Ramesh, G. Das, A solo fluorogenic probe for the real-time sensing of SO_3^{2-} and SO_4^{2-}/HSO_4^- in aqueous medium and live cells by distinct turn-on emission signals, Chem. Commun. 52 (2016) 10381–10384.
[35] S. Samanta, S. Halder, P. Dey, U. Manna, A. Ramesh, G. Das, A ratiometric fluorogenic probe for the real-time detection of SO_3^{2-} in aqueous medium: application in a cellulose paper based device and potential to sense SO_3^{2-} in mitochondria, Analyst 143 (2018) 250–257.
[36] S. Samanta, S. Halder, G. Das, Twisted-intramolecular-charge-transfer-based turn-on fluorogenic nanoprobe for real-time detection of serum albumin in physiological conditions, Anal. Chem. (2018), https://doi.org/10.1021/acs.analchem.8b01181.
[37] J. Yin, Y. Kwon, D. Kim, D. Lee, G. Kim, Y. Hu, J.H. Ryu, J. Yoon, Cyanine-based fluorescent probe for highly selective detection of glutathione in cell cultures and live mouse tissues, J. Am. Chem. Soc. 136 (2014) 5351–5358.
[38] Z. Yang, J.H. Lee, H.M. Jeon, J.H. Han, N. Park, Y. He, H. Lee, K.S. Hong, C. Kang, J. S. Kim, Folate-based near-infrared fluorescent theranostic gemcitabine delivery, J. Am. Chem. Soc. 135 (2013) 11657–11662.
[39] R. Weissleder, V. Ntziachristos, Shedding light onto live molecular targets, Nat. Med. 9 (2003) 123–128.
[40] R. Weissleder, A clearer vision for in vivo imaging, Nat. Biotechnol. 19 (2001) 316–317.
[41] J.O. Escobedo, O. Rusin, S. Lim, R.M. Strongin, NIR dyes for bioimaging applications, Curr. Opin. Chem. Biol. 14 (2010) 64–70.
[42] A. Samanta, M. Vendrell, R. Das, Y.T. Chang, Development of photostable near-infrared cyanine dyes, Chem. Commun. 46 (2010) 7406–7408.
[43] X.M. Wu, S. Chang, X.R. Sun, Z.Q. Guo, Y.S. Li, J.B. Tang, Y.Q. Shen, J.L. Shi, H. Tian, W.H. Zhu, Constructing a NIR silica-cyanine hybrid nanocomposite for bioimaging in vivo: a breakthrough in photo-stability and bright fluorescence with a large Stokes shift, Chem. Sci. 4 (2013) 1221–1228.
[44] E. Deniz, M. Tomasulo, J. Cusido, I. Yildiz, M. Petriella, M.L. Bossi, S. Sortino, F. M. Raymo, Photoactivatable fluorophores for super-resolution imaging based on oxazine auxochromes, J. Phys. Chem. C 116 (2012) 6058–6068.
[45] A.V. Anzalone, Z.X. Chen, V.W. Cornish, Synthesis of photoactivatable azido-acyl caged oxazine fluorophores for live-cell imaging, Chem. Commun. 52 (2016) 9442–9445.
[46] M. Heilemann, S. van de Linde, A. Mukherjee, M. Sauer, Super-resolution imaging with small organic fluorophores, Angew. Chem. Int. Ed. 48 (2009) 6903–6908.
[47] J. Vogelsang, C. Steinhauer, C. Forthmann, I.H. Stein, B. Person-Skegro, T. Cordes, P. Tinnefeld, Make them blink: probes for super-resolution microscopy, ChemPhysChem 11 (2010) 2475–2490.
[48] S. van de Linde, I. Krstic, T. Prisner, S. Doose, M. Heilemann, M. Sauer, Photoinduced formation of reversible dye radicals and their impact on super-resolution imaging, Photochem. Photobiol. Sci. 10 (2011) 499–506.
[49] S. van de Linde, M. Sauer, How to switch a fluorophore: from undesired blinking to controlled photoswitching, Chem. Soc. Rev. 43 (2014) 1076–1087.
[50] T.J. Mitchison, K.E. Sawin, J.A. Theriot, K. Gee, A. Mallavarapu, Caged fluorescent probes, Methods Enzymol. 291 (1998) 63–78.
[51] M.C. DeRosa, R.J. Crutchley, Photosensitized singlet oxygen and its applications, Coord. Chem. Rev. 233 (2002) 351–371.
[52] A. Kishino, T. Yanagida, Force measurements by micromanipulation of a single actin filament by glass needles, Nature 334 (1988) 74–76.
[53] M.A. van Dijk, L.C. Kapitein, J. van Mameren, C.F. Schmidt, E.J.G. Peterman, Combining optical trapping and single-molecule fluorescence spectroscopy: enhanced photobleaching of fluorophores, J. Phys. Chem. B 108 (2004) 6479–6484.
[54] M. Heilemann, E. Margeat, R. Kasper, M. Sauer, P. Tinnefeld, Carbocyanine dyes as efficient reversible single-molecule optical switch, J. Am. Chem. Soc. 127 (2005) 3801–3806.
[55] I. Rasnik, S.A. McKinney, T. Ha, Nonblinking and long-lasting single-molecule fluorescence imaging, Nat. Methods 3 (2006) 891–893.
[56] J. Widengren, A. Chmyrov, C. Eggeling, P.A. Lofdahl, C.A. Seidel, Strategies to improve photostabilities in ultrasensitive fluorescence spectroscopy, J. Phys. Chem. A 111 (2007) 429–440.
[57] A. Chmyrov, T. Sanden, J. Widengren, Iodide as a fluorescence quencher and promoter-mechanisms and possible implications, J. Phys. Chem. B 114 (2010) 11282–11291.
[58] H. Giloh, J.W. Sedat, Fluorescence microscopy: reduced photobleaching of rhodamine and fluorescein protein conjugates by n-propyl gallate, Science 217 (1982) 1252–1255.
[59] C. Steinhauer, C. Forthmann, J. Vogelsang, P. Tinnefeld, Superresolution microscopy on the basis of engineered dark states, J. Am. Chem. Soc. 130 (2008) 16840–16841.
[60] K. Valnes, P. Brandtzaeg, Retardation of immunofluorescence fading during microscopy, J. Histochem. Cytochem. 33 (1985) 755–761.
[61] N. Olivier, D. Keller, V.S. Rajan, P. Gonczy, S. Manley, Simple buffers for 3D STORM microscopy, Biomed. Opt. Express 4 (2013) 885–899.
[62] P.S. Dittrich, P. Schwille, Photobleaching and stabilization of fluorophores used for single-molecule analysis with one- and two-photon excitation, Appl. Phys. B 73 (2001) 829–837.
[63] T. Kottke, S. van de Linde, M. Sauer, S. Kakorin, M. Heilemann, Identification of the product of photoswitching of an oxazine fluorophore using fourier transform infrared difference spectroscopy, J. Phys. Chem. Lett. 1 (2010) 3156–3159.
[64] M. Irie, Photochromism: Memories and switches-introduction, Chem. Rev. 100 (2000) 1683–1684.
[65] M. Bates, T.R. Blosser, X. Zhuang, Short-range spectroscopic ruler based on a single-molecule optical switch, Phys. Rev. Lett. 94 (2005) 108101.
[66] C.R. Sabanayagam, J.S. Eid, A. Meller, Long time scale blinking kinetics of cyanine fluorophores conjugated to DNA and its effect on Forster resonance energy transfer, J. Chem. Phys. 123 (2005) 224708.
[67] J.C. Vaughan, G.T. Dempsey, E. Sun, X.W. Zhuang, Phosphine quenching of cyanine dyes as a versatile tool for fluorescence microscopy, J. Am. Chem. Soc. 135 (2013) 1197–1200.
[68] K. Kundu, S.F. Knight, N. Willett, S. Lee, W.R. Taylor, N. Murthy, Hydrocyanines: a class of fluorescent sensors that can image reactive oxygen species in cell culture, tissue and in vivo, Angew. Chem. Int. Ed. 48 (2009) 299–303.
[69] J.C. Vaughan, S. Jia, X.W. Zhuang, Ultrabright photoactivatable fluorophores created by reductive caging, Nat. Methods 9 (2012) 1181–1184.
[70] L. Carlini, A. Benke, L. Reymond, G. Lukinavicius, S. Manley, Reduced dyes enhance single-molecule localization density for live superresolution imaging, ChemPhysChem 15 (2014) 750–755.
[71] J. Vogelsang, T. Cordes, C. Forthmann, C. Steinhauer, P. Tinnefeld, Controlling the fluorescence of ordinary oxazine dyes for single-molecule switching and superresolution microscopy, PNAS 106 (2009) 8107–8112.
[72] N. Olivier, D. Keller, P. Gonczy, S. Manley, Resolution doubling in 3D-STORM imaging through improved buffers, PLoS One 8 (2013) e69004.
[73] S.J. Lord, N.R. Conley, H.L. Lee, S.Y. Nishimura, A.K. Pomerantz, K.A. Willets, Z. Lu, H. Wang, N. Liu, R. Samuel, R. Weber, A. Semyonov, M. He, R.J. Twieg, W.E. Moerner, DCDHF fluorophores for single-molecule imaging in cells, ChemPhysChem 10 (2009) 55–65.
[74] V.N. Belov, G.Y. Mitronova, M.L. Bossi, V.P. Boyarskiy, E. Hebisch, C. Geisler, K. Kolmakov, C.A. Wurm, K.I. Willig, S.W. Hell, Masked rhodamine dyes of five principal colors revealed by photolysis of a 2-diazo-1-indanone caging group: synthesis, photophysics and light microscopy applications, Chem. Eur. J. 20 (2014) 13162–13173.
[75] V.N. Belov, C.A. Wurm, V.P. Boyarskiy, S. Jakobs, S.W. Hell, Rhodamines NN: a novel class of caged fluorescent dyes, Angew. Chem. Int. Ed. 49 (2010) 3520–3523.
[76] D. Maurel, S. Banala, T. Laroche, K. Johnsson, Photoactivatable and photoconvertible fluorescent probes for protein labelling, ACS Chem. Biol. 5 (2010) 507–516.
[77] L.M. Wysocki, J.B. Grimm, A.N. Tkachuk, T.A. Brown, E. Betzig, L.D. Lavis, Facile and general synthesis of photoactivatable xanthene dyes, Angew. Chem. Int. Ed. 50 (2011) 11206–11209.
[78] P. Klan, T. Solomek, C.G. Bochet, A. Blanc, R. Givens, M. Rubina, V. Popik, A. Kostikov, J. Wirz, Photoremovable protecting groups in chemistry and biology: reaction mechanisms and efficacy, Chem. Rev. 113 (2013) 119–191.
[79] J.B. Grimm, A.J. Sung, W.R. Legant, P. Hulamm, S.M. Matlosz, E. Betzig, L.D. Lavis, Carbofluoresceins and carborhodamines as scaffolds for high-contrast fluorogenic probes, ACS Chem. Biol. 8 (2013) 1303–1310.
[80] R. Zondervan, F. Kulzer, S.B. Orlinskii, M. Orrit, Photoblinking of rhodamine 6G in poly(vinyl alcohol): radical dark state formed through the triplet, J. Phys. Chem. A 107 (2003) 6770–6776.
[81] T. Klein, A. Loschberger, S. Proppert, S. Wolter, S.V. van de Linde, M. Sauer, Live-cell dSTORM with SNAP-tag fusion proteins, Nat. Methods 8 (2011) 7–9.
[82] T. Ha, P. Tinnefeld, Photophysics of fluorescent probes for single-molecule biophysics and super-resolution imaging, Ann. Rev. Phys. Chem. 63 (2012) 595–617.
[83] R.M. Hoffman, The multiple uses of fluorescent proteins to visualize cancer in vivo, Nat. Rev. Cancer 5 (2005) 796–806.
[84] R.M. Hoffman, Imaging in mice with fluorescent proteins: from macro to subcellular, Sensors (Basel) 8 (2008) 1157–1173.
[85] M. Yang, P. Jiang, R.M. Hoffman, Whole-body subcellular multicolor imaging of tumor-host interaction and drug response in real time, Cancer Res. 67 (2007) 5195–5200.
[86] L. Stryer, R.P. Haugland, Energy transfer – a spectroscopic ruler, PNAS 58 (1967) 719–726.
[87] T. Ha, T. Enderle, D.F. Ogletree, D.S. Chemla, P.R. Selvin, S. Weiss, Probing the interaction between two single molecules: fluorescence resonance energy transfer between a single donor and a single acceptor, PNAS 93 (1996) 6264–6268.
[88] T. Ha, X.W. Zhuang, H.D. Kim, J.W. Orr, J.R. Williamson, S. Chu, Ligand-induced conformational changes observed in single RNA molecules, PNAS 96 (1999) 9077–9082.
[89] B.N.G. Giepmans, S.R. Adams, M.H. Ellisman, R.Y. Tsien, Review – the fluorescent toolbox for assessing protein location and function, Science 312 (2006) 217–224.
[90] G. Donnert, J. Keller, C.A. Wurm, S.O. Rizzoli, V. Westphal, A. Schonle, R. Jahn, S. Jakobs, C. Eggeling, S.W. Hell, Two-color far-field fluorescence nanoscopy, Biophys. J . 92 (2007) L67–L69.

[91] M. Bates, B. Huang, G.T. Dempsey, X.W. Zhuang, Multicolor super-resolution imaging with photo-switchable fluorescent probes, Science 317 (2007) 1749–1753.
[92] B. Huang, S.A. Jones, B. Brandenburg, X.W. Zhuang, Whole-cell 3D STORM reveals interactions between cellular structures with nanometer-scale resolution, Nat. Methods 5 (2008) 1047–1052.
[93] M. Bates, G.T. Dempsey, K.H. Chen, X.W. Zhuang, Multicolor super-resolution fluorescence imaging via multi-parameter fluorophore detection, ChemPhysChem 13 (2012) 99–107.
[94] H. Bock, C. Geisler, C.A. Wurm, C. Von Middendorff, S. Jakobs, A. Schonle, A. Egner, S.W. Hell, C. Eggeling, Two-color far-field fluorescence nanoscopy based on photoswitchable emitters, Appl. Phys. B 88 (2007) 161–165.
[95] H. Shroff, C.G. Galbraith, J.A. Galbraith, H. White, J. Gillette, S. Olenych, M.W. Davidson, E. Betzig, Dual-color superresolution imaging of genetically expressed probes within individual adhesion complexes, PNAS 104 (2007) 20308–20313.
[96] M. Bossi, J. Folling, V.N. Belov, V.P. Boyarskiy, R. Medda, A. Egner, C. Eggeling, A. Schonle, S.W. Hell, Multicolor far-field fluorescence nanoscopy through isolated detection of distinct molecular species, Nano Lett. 8 (2008) 2463–2468.
[97] V.N. Belov, M.L. Bossi, J. Folling, V.P. Boyarskiy, S.W. Hell, Rhodamine spiroamides for multicolor single-molecule switching fluorescent nanoscopy, Chem. Eur. J. 15 (2009) 10762–10776.
[98] M. Heilemann, S. van de Linde, M. Schuttpelz, R. Kasper, B. Seefeldt, A. Mukherjee, P. Tinnefeld, M. Sauer, Subdiffraction-resolution fluorescence imaging with conventional fluorescent probes, Angew. Chem. Int. Ed. 47 (2008) 6172–6176.
[99] S. van de Linde, U. Endesfelder, A. Mukherjee, M. Schuttpelz, G. Wiebusch, S. Wolter, M. Heilemann, M. Sauer, Multicolor photoswitching microscopy for subdiffraction-resolution fluorescence imaging, Photochem. Photobiol. Sci. 8 (2009) 465–469.
[100] A. Lampe, V. Haucke, S.J. Sigrist, M. Heilemann, J. Schmoranzer, Multi-colour direct STORM with red emitting carbocyanines, Biol. Cell 104 (2012) 229–237.
[101] M. Lehmann, B. Gottschalk, D. Puchkov, P. Schmieder, S. Schwagerus, C.P. Hackenberger, V. Haucke, J. Schmoranzer, Multicolor caged dSTORM resolves the ultrastructure of synaptic vesicles in the brain, Angew. Chem. Int. Ed. 54 (2015) 13230–13235.
[102] M. Lehmann, G. Lichtner, H. Klenz, J. Schmoranzer, Novel organic dyes for multicolor localization-based super-resolution microscopy, J. Biophotonics 9 (2016) 161–170.
[103] B. Huang, W. Wang, M. Bates, X. Zhuang, Three-dimensional super-resolution imaging by stochastic optical reconstruction microscopy, Science 319 (2008) 810–813.
[104] S.A. Jones, S.H. Shim, J. He, X. Zhuang, Fast, three-dimensional super-resolution imaging of live cells, Nat. Methods 8 (2011) 499–505.
[105] G. Shtengel, J.A. Galbraith, C.G. Galbraith, J. Lippincott-Schwartz, J.M. Gillette, S. Manley, R. Sougrat, C.M. Waterman, P. Kanchanawong, M.W. Davidson, R.D. Fetter, H.F. Hess, Interferometric fluorescent super-resolution microscopy resolves 3D cellular ultrastructure, PNAS 106 (2009) 3125–3130.
[106] D. Aquino, A. Schonle, C. Geisler, C.V. Middendorff, C.A. Wurm, Y. Okamura, T. Lang, S.W. Hell, A. Egner, Two-color nanoscopy of three-dimensional volumes by 4Pi detection of stochastically switched fluorophores, Nat. Methods 8 (2011) 353–359.
[107] K. Xu, H.P. Babcock, X. Zhuang, Dual-objective STORM reveals three-dimensional filament organization in the actin cytoskeleton, Nat. Methods 9 (2012) 185–188.
[108] S.R.P. Pavani, M.A. Thompson, J.S. Biteen, S.J. Lord, N. Liu, R.J. Twieg, R. Piestun, W.E. Moerner, Three-dimensional, single-molecule fluorescence imaging beyond the diffraction limit by using a double-helix point spread function, PNAS 106 (2009) 2995–2999.
[109] R. Wombacher, M. Heidbreder, S. van de Linde, M.P. Sheetz, M. Heilemann, V. W. Cornish, M. Sauer, Live-cell super-resolution imaging with trimethoprim conjugates, Nat. Methods 7 (2010) 717–719.
[110] A. Benke, S. Manley, Live-cell dSTORM of cellular DNA based on direct DNA labelling, ChemBioChem 13 (2012) 298–301.
[111] S.H. Shim, C. Xia, G. Zhong, H.P. Babcock, J.C. Vaughan, B. Huang, X. Wang, C. Xu, G.Q. Bi, X. Zhuang, Super-resolution fluorescence imaging of organelles in live cells with photoswitchable membrane probes, PNAS 109 (2012) 13978–13983.
[112] G. Lukinavicius, K. Umezawa, N. Olivier, A. Honigmann, G. Yang, T. Plass, V. Mueller, L. Reymond, I.R. Correa Jr., Z.G. Luo, C. Schultz, E.A. Lemke, P. Heppenstall, C. Eggeling, S. Manley, K. Johnsson, A near-infrared fluorophore for live-cell super-resolution microscopy of cellular proteins, Nat. Chem. 5 (2013) 132–139.
[113] S.N. Uno, M. Kamiya, T. Yoshihara, K. Sugawara, K. Okabe, M.C. Tarhan, H. Fujita, T. Funatsu, Y. Okada, S. Tobita, Y. Urano, A spontaneously blinking fluorophore based on intramolecular spirocyclization for live-cell super-resolution imaging, Nat. Chem. 6 (2014) 681–689.
[114] C. Flors, C.N. Ravarani, D.T. Dryden, Super-resolution imaging of DNA labelled with intercalating dyes, ChemPhysChem 10 (2009) 2201–2204.
[115] C. Flors, Photoswitching of monomeric and dimeric DNA-intercalating cyanine dyes for super-resolution microscopy applications, Photochem. Photobiol. Sci. 9 (2010) 643–648.
[116] A. Loschberger, S. van de Linde, M.C. Dabauvalle, B. Rieger, M. Heilemann, G. Krohne, M. Sauer, Super-resolution imaging visualizes the eightfold symmetry of gp210 proteins around the nuclear pore complex and resolves the central channel with nanometer resolution, J. Cell Sci. 125 (2012) 570–575.
[117] J.H. van der Velde, E. Ploetz, M. Hiermaier, J. Oelerich, J.W. de Vries, G. Roelfes, T. Cordes, Mechanism of intramolecular photostabilization in self-healing cyanine fluorophores, ChemPhysChem 14 (2013) 4084–4093.
[118] A.T. Szczurek, K. Prakash, H.K. Lee, D.J. Zurek-Biesiada, G. Best, M. Hagmann, J. W. Dobrucki, C. Cremer, U. Birk, Single molecule localization microscopy of the distribution of chromatin using Hoechst and DAPI fluorescent probes, Nucleus-Austin 5 (2014) 331–340.
[119] D. Zurek-Biesiada, A.T. Szczurek, K. Prakash, G.K. Mohana, H.K. Lee, J.Y. Roignant, U.J. Birk, J.W. Dobrucki, C. Cremer, Localization microscopy of DNA in situ using Vybrant(®) DyeCycle™ Violet fluorescent probe: a new approach to study nuclear nanostructure at single molecule resolution, Exp. Cell Res. 343 (2016) 97–106.
[120] C. Liu, J.Z. Du, L.P. Xie, R.Q. Zhang, Direct observation of nacre proteins in the whole calcite by super resolution microscopy reveals diverse occlusion patterns, Cryst. Growth Des. 17 (2017) 1966–1976.